Dynamic magnetic resonance imaging in the assessment of myocardial infarct

Einar Hopp

Department of Radiology and Nuclear Medicine

Oslo University Hospital, Rikshospitalet

University of Oslo

Oslo, Norway

Series of dissertations submitted to the
Faculty of Medicine, University of Oslo
No. 1698

ISBN 978-82-8264-620-8

Cover: Inger Sandved Anfinsen.
Printed in Norway: AIT Oslo AS.

Produced in co-operation with Akademika Publishing.
The thesis is produced by Akademika Publishing merely in connection with the thesis defence. Kindly direct all inquiries regarding the thesis to the copyright holder or the unit which grants the doctorate.

To Hanne and Ulrik

Good judgment is the result of experience, and experience the result of bad judgment.

- Mark Twain

Contents

Acknowledgements

The present work was conducted during the years 2005 – 2013 at the Department of Radiology and Nuclear Medicine at Oslo University Hospital, Rikshospitalet. For 5 years I was supported as a part-time researcher at the Department, and for 6 months I received a research fellowship from Helse Sør-Øst. I am grateful for all support.

A lot of people have made this work possible. I wish to express my sincere gratitude to

– my primary supervisor Hans-Jørgen Smith for teaching me cardiac MRI and medical research, and my co-supervisor Thor Edvardsen for sharing his comprehensive knowledge of clinical cardiology, imaging and research. Both have been available for any purpose and have practiced a perfect balance of encouragement and constructive criticism.

– my additional co-authors; Atle Bjørnerud, Svend Aakhus, Ola Gjesdal, Ketil Lunde, Svein Solheim, Kolbjørn Forfang, Harald Arnesen, Halfdan Ihlen, Trond Vartdal and Thomas Helle-Valle. All have made unique and fruitful contributions to the work.

– my different leaders throughout the research period; Bjarne Smevik, Andreas Abildgaard, Heidi Eggesbø and Paulina Due-Tønnessen for their encouragement and struggle for research resources

– all my colleagues at Pediatric Imaging, General Imaging and Thoracic, Vascular and ENT Imaging, successively, for always doing their best to free time for research and researchers

– the radiographers at the MR unit for excellent patient care and skillful MR imaging, their leader during my research period Eldrid Winther-Larssen for creating tradition for quality work and cardiac MRI radiographer Rolf Svendsmark for invaluable work

– secretary Jorund Roos for her engaged and never failing inclusion of patients

– my brother Petter Hopp for analytic comments on the thesis, and my friend Harald Øhrn for valuable conversations

– all patients who accepted enrolment in the studies

– and least but not last; my family at home, continuously reminding me what is most important in life.

Abbreviations

2D-STE	Two-dimensional speckle tracking echocardiography
AIF	Arterial input function
AMI	Acute myocardial infarction
ASTAMI	Autologous stem cell transplantation in acute myocardial infarction
AUC	Area under the curve
bSSFP	Balanced steady state free precession
CSPAMM	Complementary spatial modulation of magnetization
DCE	Dynamic contrast-enhanced
ε	Strain
ε_C , ε_L	Circumferential strain and longitudinal strain, respectively
EES	Extravascular, extracellular space
Gd	Gadolinium
GRE	Gradient echo
ICC	Intraclass correlation coefficient
k_{ep}	The rate constant of contrast agent vascular return
K^{trans}	The transfer constant of contrast agent extravasation
LGE	Late gadolinium enhancement
LV	Left ventricle
LV EDV	Left ventricular end-diastolic volume
LVEF	Left ventricular ejection fraction
LV ESV	Left ventricular end-systolic volume
mBMC	Mononuclear cells derived from bone marrow
MO	Microvascular obstruction
MR	Magnetic resonance
MRI	Magnetic resonance imaging
PCI	Percutaneous coronary intervention
PS product	Product of permeability and surface area of the capillary bed
PSSI	Post-systolic shortening index
rBF	Residue blood flow
RF	Radiofrequency
ROC	Receiver operating characteristic
ROI	Region of interest
SD	Standard deviation
SPAMM	Spatial modulation of magnetization
STEMI	ST-segment elevation acute myocardial infarction
TBF	Tissue blood flow
TIC	Time intensity curve
TTP, TTP_i , TTP_n	Time to peak and time to peak for infarct tissue and normal tissue, respectively
v_e	Extravascular, extracellular space volume fraction
WMS(I)	Wall motion score (index)

List of papers

I Hopp E, Lunde K, Solheim S, Aakhus S, Arnesen H, Forfang K, Edvardsen T, Smith HJ. Regional myocardial function after intracoronary bone marrow cell injection in reperfused anterior wall infarction - a cardiovascular magnetic resonance tagging study. *J Cardiovasc Magn Reson* 2011; **13**:22.

II Hopp E, Bjørnerud A, Lunde K, Solheim S, Aakhus S, Arnesen H, Forfang K, Edvardsen T, Smith HJ. Perfusion MRI at rest in subacute and chronic myocardial infarct. *Acta Radiol* 2013; [Epub ahead of print].

III Gjesdal O, Hopp E, Vartdal T, Lunde K, Helle-Valle T, Aakhus S, Smith HJ, Ihlen H, Edvardsen T. Global longitudinal strain measured by two-dimensional speckle tracking echocardiography is closely related to myocardial infarct size in chronic ischaemic heart disease. *Clin Sci (Lond)* 2007; **113**(6):287-296.

1 Introduction

1.1 Coronary heart disease

Coronary heart disease is a major cause for morbidity and mortality throughout the world[1;2]. Owing to improved prevention, diagnosis and treatment, death rates have declined in North America and Western European countries[3]. Milestones include the identification of risk factors like smoking, high blood pressure and blood cholesterol, the emphasizing of early identification and treatment of heart attack, and treatment options like medication, percutaneous coronary intervention (PCI) and intensive care for the critically ill heart failure patient[3].

Myocardial infarction is caused by interrupted blood supply to a part of the heart muscle, most commonly after occlusion of a coronary artery. After acute myocardial infarction (AMI) myocardial tissue goes through a process of necrosis, edema and inflammation, followed by fibroblast invasion and proliferation and the eventual scar formation with dense fibrous tissue without myocardial cell repair[4;5]. The scar is characterized by thinning, elongation and reduced contraction, while the remaining undamaged part of the myocardium may change with hypertrophy and increased contraction. Especially in large, transmural infarcts of the left ventricle (LV) there is risk of development of adverse remodeling, characterized by left ventricular enlargement, altered geometry and development of congestive heart failure[4;6].

1.2 Stem cell treatment in myocardial infarct

At the turn of the millennium, reports on myocardial cell regeneration from bone marrow cells emerged[7;8]. Several clinical trials were initiated to explore the potential for myocardial cell repair from stem cells in a clinical setting[9-13]. In Oslo, the Autologous Stem Cell Transplantation in Acute Myocardial Infarct (ASTAMI) study was started in 2003, recruiting patients with AMI from Rikshospitalet University Hospital and Ullevål University Hospital[14]. The purpose was to assess whether stem cell therapy after AMI could facilitate relative preservation of LV function.

1.3 Imaging-based judgment of the infarcted left ventricle

1.3.1 Global left ventricular function

The vast majority of myocardial infarcts affect the free wall of the LV or septum and in the chronic phase the main interest is the LV function. A local damage directly influences the capability of the LV to compress and eject sufficient stroke volume. The global LV ejection fraction (LVEF) is the most commonly used measurement for characterization of the LV function. Reduced LVEF is correlated to mortality and is still one of the most important prognostic determinants after myocardial infarct [15]. The calculation is based on measurements of end diastolic and end systolic volumes. The result is given in percent from the equation

$$LVEF = \frac{EDV - ESV}{EDV} \times 100 \tag{1}$$

where EDV is end diastolic volume and ESV is end systolic volume. The LV may dilate with increasing EDV and ESV, compensating reduced LVEF with the preservation of stroke volume. The global LV function results from the sum of regional contraction. In spite of local damage, LVEF may be preserved. Thus, assessment of regional wall function adds more detailed information on LV function and even prognosis after myocardial infarct[16].

1.3.2 Regional function

Correct anatomical assignment of myocardial segments is crucial for comparison of regional analysis between individuals and from one method to another. Currently, the 17 segment model is most often used[17]. Some advantages of the model are the simplicity, the standardization of image planes combined with segmentation, standardization across modalities and a model for coronary perfusion territories. For long, qualitative assessment of regional wall motion has been performed with scoring as normal, hypokinetic, akinetic or even dyskinetic with a diversity of methods[18]. Regional wall motion score (WMS) further indexed represents an LV wall motion score index (WMSI)[19].

Strain is defined as stress-induced relative deformation from the original or unstressed dimensions. The introduction of this deformation parameter increased the

ability to quantify regional movement of the LV[20]. The parameter is dimensionless, as deformation is viewed in relation to the initial length, but with a principal direction and may be expressed as a vector. Lagrangian strain is defined as deformation fraction:

$$\varepsilon = \frac{L - L_0}{L_0} \tag{2}$$

where ε is Lagrangian strain, L = instantaneous length and L_0 = initial length. Thus, shortening is negative ε, and thickening is positive. Strain rate is the time derivate of ε, measured in s^{-1} or 1/s. For one- or two-dimensional imaging systems ε has to be projected (Figure 1). In severe ischemia marked changes of local deformation patterns occur, with stretching during iso-volumetric contraction and shortening during early diastolic phase of dyskinetic regions[21]. Thus, studies on regional deformation with sufficient temporal differentiation enables even more detailed characterization of myocardial dysfunction.

Figure 1: Strain projections

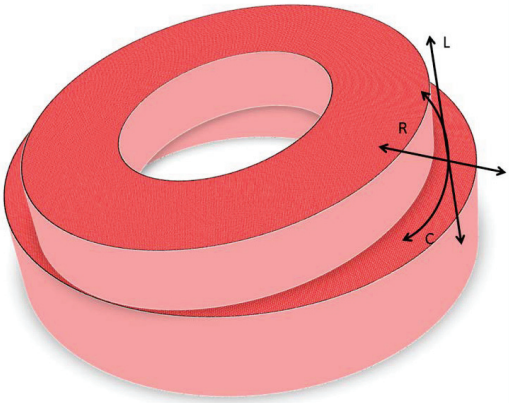

Projection of myocardial ε measurement into one of three directions, as viewed in relation to the LV wall. ε_L is deformation along the wall from base to apex (L). ε_C is the deformation of the short axis circle (C), whereas ε_R defines the thickening or thinning of the ventricular wall parallel to the short axis diameter (R).

The myocardial structure of the LV is complex with the muscle wall organized in layers of different myofibrillar orientation. The inner, subendocardial layer and the outer, subepicardial layer form a couple of two opposite orientated helix bands, and between them there is a circumferentially orientated layer. The oblique fiber angle favors contraction and the ability to withstand wall stress. The anatomical architecture also explains the torsion of the ventricle with a counter-clockwise rotation of the apical part, as viewed from the apex, and the opposite rotation in the

basal part[22]. Tissue tracking methods have made it possible to follow the more complex, wringing movements of the LV, and calculate the magnitude of counter-clockwise torsion of the apical part as seen from the apex, or the difference between the apical torsion and the opposite basal torsion (LV twist)[23-25].

1.3.3 Tissue perfusion and microvascular obstruction

Tissue perfusion provides delivery of nutrition and O_2 and clearance of CO_2 and heat. Metabolism depends on sufficient microcirculation which is influenced by reduced coronary flow and might be altered in a variety of myocardial diseases including ischemia, infarct, inflammation and repair. Perfusion imaging is the registration of perfusion dependent tissue change over time, and is used for assessment of ischemia or microvascular disease. Classically, a diffusible tracer in the vascular bed is exchanged between the vascular compartment and tissue and influences characteristics of tissue imaging. A slice or a volume is repeatedly scanned for the visual registration of tissue differences due to tracer level inhomogeneity, or even a time curve with more quantitative regional scaling of the tracer is generated.

Stress perfusion imaging is by far the most common cardiac perfusion imaging acquisition. Stress is induced either with physical activity or pharmacologically; as vasodilator or ionotropic stress. The purpose is to achieve maximum coronary flow for the revelation of ischemia due to coronary stenosis, qualitatively assessed from reduced tracer quantities during first pass, reversible at rest. The method is considered a powerful non-invasive diagnostic tool in the work-out of suspected coronary ischemic disease[26;27].

Commonly, acute or chronic infarct zones are shown to be hypoperfused during first pass of a tracer such as a contrast agent. The term microvascular obstruction (MO) designates a more prolonged or permanent hypoenhancement of the contrast medium in the core of a reperfused myocardial infarct. MO has been closely linked to the no-reflow or low-reflow phenomenon[28;29]. This phenomenon describes a zone of severely reduced flow in the infarct core in more extensively damaged tissue after prolonged ischemia and reperfusion. Capillary damage and small vessel obstruction have been suggested the major contributing factors of the phenomenon, possibly with

a role for blood viscosity[30]. Presence of MO is invariably related to larger infarct size and is considered an independent prognostic factor for adverse remodeling or cardiovascular events[31-33].

The natural course is not described in detail. MO may be present immediately after the infarct. In dogs, MO increases over the first 48 hours after the incident[29;34] and is present for several days[35]. In humans, the phenomenon has mainly been studied during the first week after AMI[31;32;36-38]; in a longitudinal study the number of patients with MO decreased from 2 days to 7 days after PCI, and the phenomenon was gone at 2 months[33].

1.3.4 Infarct visualization

Direct in vivo visualization of myocardial infarct tissue is dependent on altered cellular activity or tissue composition. Techniques of nuclear medicine are primarily based on cellular metabolism. The late gadolinium enhancement (LGE) technique of cardiac MRI is based on the increased extracellular volume in acute or chronic infarcts. LGE may not be specific per se, with the possible confusion with inflammatory tissue. Infarct size and transmurality are independently correlated to severity of the remodeling process[4;38;39], thus precise anatomical characterization of the infarct supplies useful information for risk stratification and therapeutic monitoring. The superior spatial resolution of MRI is an advantage, making precise transmurality assessment possible. Grading of transmurality can be performed in two principally different ways. *Transmural extent* is maximum transmurality of the infarct, as extent of the complete wall thickness, for example if the infarct affects less than or more than half of the complete wall thickness in a segment or perfusion territory. In computerized systems this grading has been averaged over a complete segment or area[40;41]. The other grading system is the *percent scar*[42] of a segment or area. The two systems have been shown to score similarly with reference to ε_C[43]. In several studies transmurality has been classified as an ordinal parameter with transmural extent or percent scar in groups; most often categorized from 1 to 4 representing increasing quartiles with no infarct classified as 0.

1.4 Magnetic resonance imaging

Imaging modalities are techniques used for medical imaging. Examples are MRI, echocardiography, computed tomography, x-ray and fluoroscopy and a range of nuclear medicine techniques. MRI does not use ionizing radiation; it transforms differences in tissue magnetization into images by means of a very strong magnet, applied magnetic field gradients and transmitted radiofrequency (RF) pulses.

1.4.1 Motion

The movements of the heart make demands on short acquisition time, which in turn challenges additional MRI properties. An image of the beating heart has to be captured in small fractions of a second. To achieve time for enough phase encoding steps, the routine cardiac MRI sequence samples data at particular time points of the cardiac cycle for several cardiac cycles. The cardiac MRI sequence is synchronized with the the patient's ECG sampled simultaneously[44]. An anatomical image is the result of sampling from the similar equal delays after the "R" wave from several cardiac cycles. A series of images sampled at multiple time points, each image always at the same time point, in sum appear like a series of images from one cardiac cycle. This sampling at multiple time points of the heart cycle allows viewing of the series in a movie, known as a cine sequence. ECG triggering may be prospective (RF-pulse initiated immediately after the "R"-wave) or retrospective which is useful when there are small beat-to-beat variations of the heart interval[45].

Image acquisition in cardiac MRI is commonly performed during breath-hold to avoid motion artifacts from respiratory movements. Another option is to sample data at the same respiratory position by respiratory gating, most often performed with an edge-detecting algorithm at the lung/diaphragm border – called respiratory navigator technique[46].

1.4.2 Foreign bodies and implants

Owing to the strengths of the static and oscillating magnetic fields of the MR system, items brought into the magnet room like ferromagnetic foreign bodies or medical implants and devices, may represent hazard to the patient or other persons in the magnet room. Potential problems include objects acting like projectiles, items inside the patient getting displaced or torqued, medical devices making electric field

interactions, MRI-related heating, electromagnetic affection of the operation of an electric device or induction of currents in such, and implant-related artifacts. Undesired motion of the device is less likely with firm implantation.

Concern is about hazard to the patient, the understanding of artifacts, but also the inappropriate prevention from needed examinations. Testing methods have been established[47-50], guidelines for industry have been published[51], and comprehensive and detailed summaries on medical devices and contraindications are continuously updated[52;53]. Terminology changed in 2005. The term *MR unsafe* is for items posing hazard in any MR environment. *MR safe* is for nonconducting, nonmetallic, nonmagnetic items with no known hazard in any MR environment. *MR conditional* is for items posing no hazard in specified magnetic environments. Technical development makes it necessary to continuously control unknown medical devices and implants in updated safety guideline databases and against the manufacturer's handbooks and web pages.

Some implants are especially relevant for cardiology[54].

Sternal wires after sternotomy are MR safe. Most *aortic stent grafts* that have been tested are labeled MR safe, with an important exception regarding the Zenith AAA Endovascular Graft® with components made from stainless steel. It is classified MR conditional, and has to be controlled against characteristics of the specific magnet. *Inferior vena cava filters* are for most labeled MR safe, for some the waiting after implantation will allow firm implantation. *Coronary and peripheral vascular stents* are labeled MR safe or MR conditional if they contain ferromagnetic components. Data for high-field magnets (≥ 3.0 T) is not complete. *Embolization coils* made from nitinol, iridium and platinum are considered safe at field strengths 3.0 T and lower. Coils with ferromagnetic components are MR conditional, so allow time for firm implantation. In general, there is a theoretical potential for coil heating during examination. *Cardiac closure devices* from non-ferromagnetic materials are labeled MR safe. Again, some devices with ferromagnetic components are labeled MR conditional. *Prosthetic heart valves and annuloplasty rings* are either MR safe or for a lesser number MR conditional. In general, MR examination is not contraindicated, but there is a reservation for devices with minor ferromagnetic components in high-field magnets. Traditional *permanent cardiac pacemakers* and *implantable*

cardioverter defibrillators (ICD) contain ferromagnetic components and complex electrical systems. Potential complications are displacement, damage and dysfunction of the device and cardiac stimulation and heating of the tip. However, several implanted pacemaker patients have undergone MR examinations; sometimes unintentionally[55-57]. Very few serious complications have been reported[57-61]. At least three manufacturers now produce *MR compatible pacemakers* to be introduced in the MR environment under controlled circumstances[62-68]. Patients with *retained transvenous pacemaker and defibrillator leads* should not undergo MR examination. *Temporary cardiac pacemakers* contraindicate MR examination because of the external pulse generator. *Retained temporary epicardial pacing leads* do not pose a significant risk for MRI, at least as long as the leads are short and without large loops[69]. *Hemodynamic monitoring and hemodynamic support devices* like the Swan-Ganz catheter, ventricular assist devices and intra-aortic balloon pumps are complex electric devices which contain ferromagnetic material and leads. These devices are MR unsafe.

1.4.3 Monitoring of the critically ill patient

Cardiovascular monitoring in the MR unit is demanding and the anesthetists miss their usual access to direct patient contact. If critical illness occurs during an MR examination, either as worsening of the patient's condition or as a complication to medication during the examination, resuscitation has to be initiated in the near vicinity of the MR suite. In a life support situation, staff members are called, and emergency equipment is in use. It is of high importance that these situations are handled outside the magnet room, in order to prevent ferromagnetic objects to act like projectiles, and to prevent entering of unauthorized staff members. These circumstances, added to the fact that hemodynamic support devices are MR unsafe, reduce the general access to MR examination for unstable and critically ill patients.

1.4.4 Nephrogenic systemic fibrosis

Nephrogenic systemic fibrosis (NSF) was first diagnosed in 1997, with the first report published in 2000[70]. The skin gradually thickens; there is fibrous proliferation and thickened collagen bundles, but no inflammatory signs. Extremities are affected, followed by the torso. Lungs, liver, esophagus, heart and muscle might become

involved in patients with systemic affection. The patient may die from the disease. There is no known cure. The disease may stabilize spontaneously, but rarely remits[71].

All patients diagnosed with NSF so far, have suffered from severe renal failure, and most were in need for treatment with hemodialysis[70;71]. In 2006 the first reports on a possible connection between NSF and gadolinium (Gd) based contrast agents were published[72;73]. Although the mechanism is not clarified, it is now believed that the administration of Gd based contrast agents in patients with renal failure carries a risk for NSF development, and the risk increases with lower residual renal function[71;74;75]. Repeated administration and increased accumulated dosage of Gd increases the risk[76]. Metabolic acidosis and proinflammatory state, among other comorbidity, have been suggested to increase the risk. Incidence numbers from 3 % to 18 % have been reported among renal failure patients receiving Gd based contrast agents[77], and hemodialysis has not proven to give preventive effect[71]. Symptoms develop up to 6 months after Gd administration. Different classes of Gd chelate binding may carry different risk for the patient[78].

In this light contrast agent administration for MRI is contraindicated in patients with severe renal failure[79], but there is no known risk for patients with normal renal clearance (above 60 ml/min/1.73m^2)[80]. International guidelines and recommendations have been developed to avoid the development of the disease[80-82]. One main challenge is to identify patients with decreased renal clearance; another to avoid the inappropriate use of Gd based contrast agents.

1.5 Dynamic magnetic resonance imaging of the heart

In this respect, the meaning of the term “dynamic” is either of two:

- The image sequence displays the movements of the heart or the blood flow inside the heart and the great vessels.
- The image sequence detects myocardial signal intensity changes over time dependent on flow through the tissue; or detects signal intensity changes due to the injection of contrast agent, dependent on time from the injection.

Not all dynamic cardiac MRI is covered. MRI methods discussed in this thesis are cine imaging, tagging MRI, contrast-enhanced perfusion imaging at rest and LGE.

1.5.1 Cine imaging

1.5.1.1 Bright blood sequences

Cardiac cine MRI is a technique where a set of images at the same slice position, are acquired at several time points throughout the cardiac cycle and shown sequentially to give the impression of the beating heart. Spoiled gradient echo (GRE) and balanced steady state free precession (bSSFP) pulse sequences are used for cine imaging. In spoiled GRE inflowing blood looks bright compared to the surrounding tissue, and in bSSFP blood signal is high due to the high T2/T1 of fluid. Thus, these sequences with good contrast to stationary tissue and vessel walls have been called bright blood imaging. The signal of blood in bSSFP is much higher than in spoiled GRE, increasing the contrast. On the other hand, signal of blood is more prone to flow artifacts in the spoiled GRE sequence, making the sequence more sensitive to jets from valvular disease.

Development of the bSSFP sequence led to several comparisons between the two methods[83;84]. In short, introduction of bSSFP provided increased signal to noise ratio, increased signal contrast and improved edge detection between blood and ventricular endocard. Higher signal enabled increased spatial and temporal resolution. Visualization of dephasing of the flow due to jets and regurgitations diminished. Measures of the LV changed slightly, with higher end diastolic and end systolic volumes, lower muscular mass, but without change of LVEF[83]. Inter-study reproducibility increased with bSSFP, and utilization of semi-automatic measurement software was made feasible[84]. As a result, the bSSFP has replaced the more traditional spoiled GRE sequence for cine cardiac MRI with magnetic field strengths below 3.0 T.

1.5.1.2 Left ventricular volume measurement

A method for numerical integration, the numerical approximation of definite integrals, is called “Simpson’s rule”; after the British mathematician Thomas Simpson (1719 – 1761). Even though the areas of the different slices in a stack usually are measured independently from each other, instead of performing approximation of integrals, summing up the areas is still called Simpson’s rule. The

method is independent from geometrical presumptions and has proven robust and reproducible in engineering, in medicine, as well as cardiology[85;86].

A main advantage of cardiac MRI is the free choice of selecting any imaging plane, making imaging at reproducible cardiac axes possible. For heart volume measurement short axis slices aligned perpendicular to the LV long axis are utilized. If breath-hold is not similar from slice to slice, significant through-plane movement occurs between the slices, reducing measurement precision. This latter problem is avoided with 3D acquisition of the complete ventricular complex with multiple slices in a single breath-hold, at the cost of reduced temporal and spatial resolution.

Calculation of LV EDV and ESV, and thus LVEF, rely on the precise identification of end diastolic and end systolic frames. The endocardial border has to be identified, but with manual delineation papillary muscles are included in the luminal area for practical reasons. The precise identification of the mitral valve plane (or for the right ventricle: the tricuspid valve plane) is a crucial point due to the relatively large short axis area at the basal cut edge of the ventricle. For myocardial muscle measurements also the epicardial contour has to be drawn. In order to save time numerous automatic and semi-automatic delineation software packages have been made[87].

Alternatively, several models based on geometrical presumptions have been offered, in order to reduce number of delineated contours and calculation time. The "modified Simpson's rule" is based on the LV long axis and two short axis areas, the "biplane ellipsoid formula" was based on the LV long axis and one long and one short axis ventricular area. Other models include the "hemisphere cylinder", the "single-plane ellipsoid"[88], and the "Teichholz formula"[89]. The biplane ellipsoid model has later been based on two perpendicular long axis areas and the LV long axis[90-93]. All models have been tested to some extent with variable results[88]. As a general objection, the different geometric presumptions are believed to be more accurate in normal LVs or in LVs with global pathology than in an LV remodeled from regional myocardial pathology.

1.5.2 Cardiovascular magnetic resonance tagging

Tagging is the magnetic marking of tissue or fluid immediately followed by an MR sequence with the intention to track movement or deformation over time. By

introduction in 1988, this was the first noninvasive method to visualize transmural myocardial movement[94;95]. Most tagging techniques are still based on linear or grid demagnetization of tissue, appearing as hypodense stripes. With movement of the tissue, the lines move and deform, and the pattern and amplitude of displacement reflect tissue motion. The direct, qualitative judgment of the tagging sequence is possible, but the ability to quantify regional movement and deformation non-invasively was an important progress.

Pulse sequences and initial tissue tagging have become faster, more flexible and with higher contrast[96]. The problem of early fading of tags due to tissue remagnetization has been reduced[97]. 3D tagging sequences have been introduced[98]. Not least, semi-automatic analysis tools have been developed, thereby reducing post-processing time dramatically[99;100].

In 1989, the spatial modulation of magnetization (SPAMM) technique was introduced with a combination of two non-selective RF-pulses separated by a weak dephasing gradient pulse. The stripes had a regular pattern with a sinusoidal intensity profile[101]. The SPAMM technique was almost immediately modified with more RF-pulses of varying amplitudes, again separated by dephasing gradient pulses, thereby increasing tag contrast[102]. To overcome the problem of tag fading, the complementary spatial modulation of magnetization (CSPAMM) technique was constructed. The technique increased tagging amplitude and tissue signal at later phases; thereby increasing tag contrast and providing visualization of deformation in late diastole as well. The disadvantage was the doubling of the acquisition time[97].

Different approaches for tagging analysis have been introduced. Methods like active contour, optical flow, template matching, sinusoidal analysis and grid line detection with snakes were all characterized by long processing time[95]. In 1995 an automated Fourier based algorithm for the tracking of SPAMM tags was proposed and initially validated[103].

The harmonic phase (HARP) technique also utilized the Fourier domain in which the SPAMM tag pattern produces an underlying array of spectral peaks. The information from each of these peaks yields a complex harmonic image, and a harmonic magnitude and harmonic phase image can be reconstructed. The harmonic phase

image contains information on myocardial motion, and this motion is tracked by the analysis of the HARP angle. This tracking is principally independent from the tags, and the method reduced noise and increased resolution. When the analysis program was introduced, the HARP technique was semi-automated requiring the tracking of a subendocardial and subepicardial circle on short axis reconstructed images for the subsequent immediate estimation of radial or circumferential Lagrangian strain (ε_R and ε_C). Manual correction of erroneous tracking (tag jumping) was required. However, the post-processing time was dramatically reduced compared to earlier methods[99]. The method was further validated in experimental and patient studies[104-106]. The Multi-Ethnic Study of Atherosclerosis has demonstrated the potential for ε examinations of larger populations with the HARP tool[107-110].

1.5.3 Perfusion magnetic resonance imaging

In paper II, perfusion imaging was performed with *Dynamic contrast-enhanced imaging* (DCE MRI), which is the method to be discussed. In DCE MRI, T1-weighted images are acquired repeatedly during the infusion of a T1-enhancing contrast agent. The signal intensities of the arterial bed and subsequently the tissue are enhanced, and the dynamic signal intensity registration over time enables characterization of tissue perfusion. The consequent mathematic relationship between perfusion and signal change is, among other factors, dependent on negligible susceptibility effects from the contrast agent injected.

1.5.3.1 Technique

A fast GRE sequence after a non-selective saturation pulse has made it possible to image a stack of 3 to 5 images during each RR-interval with stable T1 contrast over a broad spectrum of contrast concentration. Later, bSSFP with shorter acquisition time and higher signal to noise ratio, and different hybrid techniques with echo-planar imaging and non-cartesian k-space trajectories have been introduced.

Contrast medium injection has to be sufficiently fast. If not, sensitivity for changes in myocardial blood flow is limited. An injection rate in the range of at least 3 ml/s is recommended. Injection dosage determines signal increase in the LV cavity and myocardial tissue[111]. A sufficiently high dose is convenient for the qualitative judgment of myocardial perfusion. The quantitative analysis of myocardial tissue

perfusion is dependent on correlation to an arterial input function (AIF) most often from the LV cavity or aortic lumen. For high concentrations, there is a non-linear relationship between contrast agent concentration and signal intensity, due to T2* effects.

The qualitative work-out of myocardial perfusion imaging is simply the visual judgment of tissue enhancement during contrast medium first pass. Regions of hypoenhancement are noticed. Quantitative analysis is the mathematical analysis of measurements of tissue enhancement during first pass or longer. The latter is based on intensity values from the time intensity curves (TICs) measured in regions of interest (ROI) of myocardial tissue and LV lumen.

The analysis of the endocardial border remains a challenge in perfusion imaging, irrespective whether analysis is qualitative or quantitative. Partial volume effects and spill over from high intensity contrast filling of the LV cavity make border tracking challenging, and may reduce thickness of measurable myocardium especially in the apical regions. More often, a so-called dark rim artifact affects reading. This artifact is transient and peaks with maximum LV contrast filling and may precede contrast arrival of myocardial tissue[112]. The artifact is reduced with increasing spatial resolution, which increases demands on image quality and may affect temporal resolution[112;113].

1.5.3.2 Quantitative assessment of dynamic contrast-enhanced MRI

Numerous perfusion parameters have been reported, with differing nomenclature. In paper II we mainly kept to one set of standardized quantities and symbols[114]. Perfusion is tissue blood flow (TBF) per mass of tissue per time, often expressed in ml/100 g/min. Tissue blood volume is the fraction of tissue volume occupied by vessels. Mean transit time is mean time for a particle to be occupied in the volume considered. Mean transit time depends on tissue blood volume, blood velocity and vascular architecture.

The central volume principle defines the relationship:

$$\tau = MTT = \frac{TBV}{TBF} \tag{3}$$

where τ and MTT denote mean transit time, TBV is tissue blood volume and TBF is tissue blood flow. Neither of these parameters is directly measurable, and we approach the calculation indirectly.

The T1 positive contrast agent rapidly injected is a water soluble tracer introduced into a fluid flowing at unknown rate through a system of unknown distribution volume. In this respect the tracer is extracellular and crosses the vascular wall rapidly and distributes into the extravascular, extracellular space (EES). With DCE MRI the effect of the tracer upon tissue signal is measured at a sampling site over appropriate time intervals, some place downstream from the injection site.

Some tissue parameters of interest are directly derived from the TIC, but have to be considered together with information from AIF. The AIF is easily accessible in myocardial perfusion imaging from the aortic or LV lumen. Peak intensity is the maximum intensity value of either AIF or tissue measured. Time to peak (TTP) is the time to the peak intensity value of the curve. Here, TTP_n and TTP_i denote normal and infarct tissue TTP, respectively. Increased tissue TTP could be an indication of arterial collateral circulation or stenosis, but has to be correlated to the contrast arrival time. Initial upslope of the curve is the direct derivation of the initial intensity rise and is related to tissue flow and contrast agent leakage. Area under the curve (AUC) is the integral of the intensity-time curve of AIF or tissue. AUC up to AIF first pass peak is closely related to tissue volume. Parameters directly derived from the TIC are called *descriptive enhancement parameters* in this work. They are influenced from individual hemodynamics and infusion variations. This latter influence acts directly through the arterial input. Hence normalization to the AIF provides the possibility for a more general understanding of descriptive enhancement parameters.

Intravascular space is the volume of the blood vessels, approximately 2-10% of different tissue volumes. The plasma volume fraction of the intravascular space is the intravascular distribution volume for intra- and extravascular contrast agents. EES is

the extravascular extracellular space; that is the interstitium excluding the intracellular space. v_e is the EES volume fraction (of the whole volume); the extravascular distribution volume for contrast agents. The MR signal is registered from a tissue voxel of known volume with unknown v_e and unknown vascular volume with unknown plasma volume fraction.

The two-compartment model

Shortly after the contrast agent has reached the vascular bed of a tissue volume, it distributes into the extravascular space. Some contrast agent returns to the vascular bed. The distribution takes some time, dependent on flow, the area and permeability of the vascular bed, and the extravascular distribution volume. K^{trans} is the transfer constant from the vascular compartment to the EES. k_{ep} is the rate constant for the reflux from the EES back to the vascular component. The relationship between these parameters is illustrated in the two-compartment model (Figure 2) and is given by equation (4):

$$k_{ep} = \frac{K^{trans}}{v_e} \tag{4}$$

A so-called mixed model describes the situation when K^{trans} is dependent on TBF, and influenced by endothelial permeability and recruitment of myocardial capillaries. P is the permeability and S is the surface area of the capillary bed, together they form the PS product. TBF and the PS product do not vary independently, as vasodilatation probably is followed by capillary recruitment and increase of the capillary bed area[115]. With limited flow and high PS product (PS >> TBF), K^{trans} is directly proportional to flow. With limited permeability and sufficient flow (TBF >> PS), K^{trans} is determined by the PS product of the capillary wall and the concentration gradient[114].

Figure 2: The two-compartment model

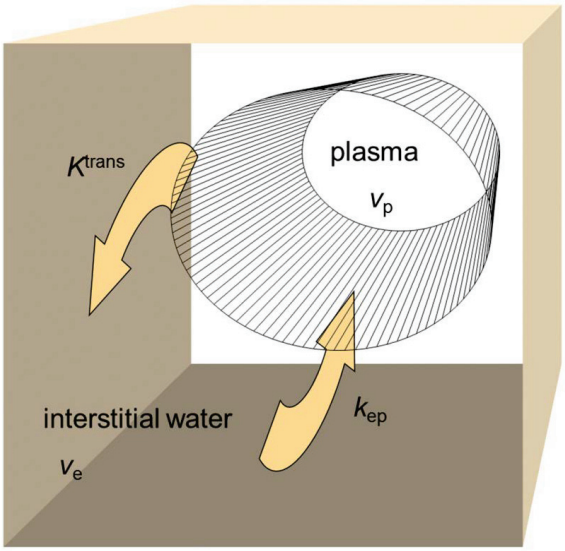

A simplified illustration of the two-compartment model for contrast agent transfer between tissue compartments

The box illustrates an arbitrary voxel of tissue and the cylinder is the sum of vessels within. An extracellular contrast agent is distributed in plasma and interstitial water and exchange between these compartments.

Deconvolution and the residue curve

The tissue concentration curve of a tracer is dependent on an idealized tissue response of a tracer bolus transferring the tissue, and the arterial input of the tracer. The relationship is described in equation (5) as the convolution of the input and the response curve[116]:

$$tissue(t) = AIF \otimes R(t) \tag{5}$$

where tissue(t) is tissue tracer concentration at time t, $\otimes$ denotes convolution and R is the response curve. Assuming a linear relationship between tracer concentration and tissue signal the residue function, resembling the response curve, can be derived from a deconvolution process of tissue TIC to AIF. Fitted signal TICs include estimates of the *kinetic parameters* K^{trans} and k_{ep} and the volume parameters v_e and plasma volume fraction (v_p). The instant, maximum value of the residue curve is an approximation to tissue flow (rBF)[117-119]. An example of tissue TICs deconvolved to AIF with the resultant residue curves is shown in Figure 3.

Figure 3: Time intensity curve and residue curve

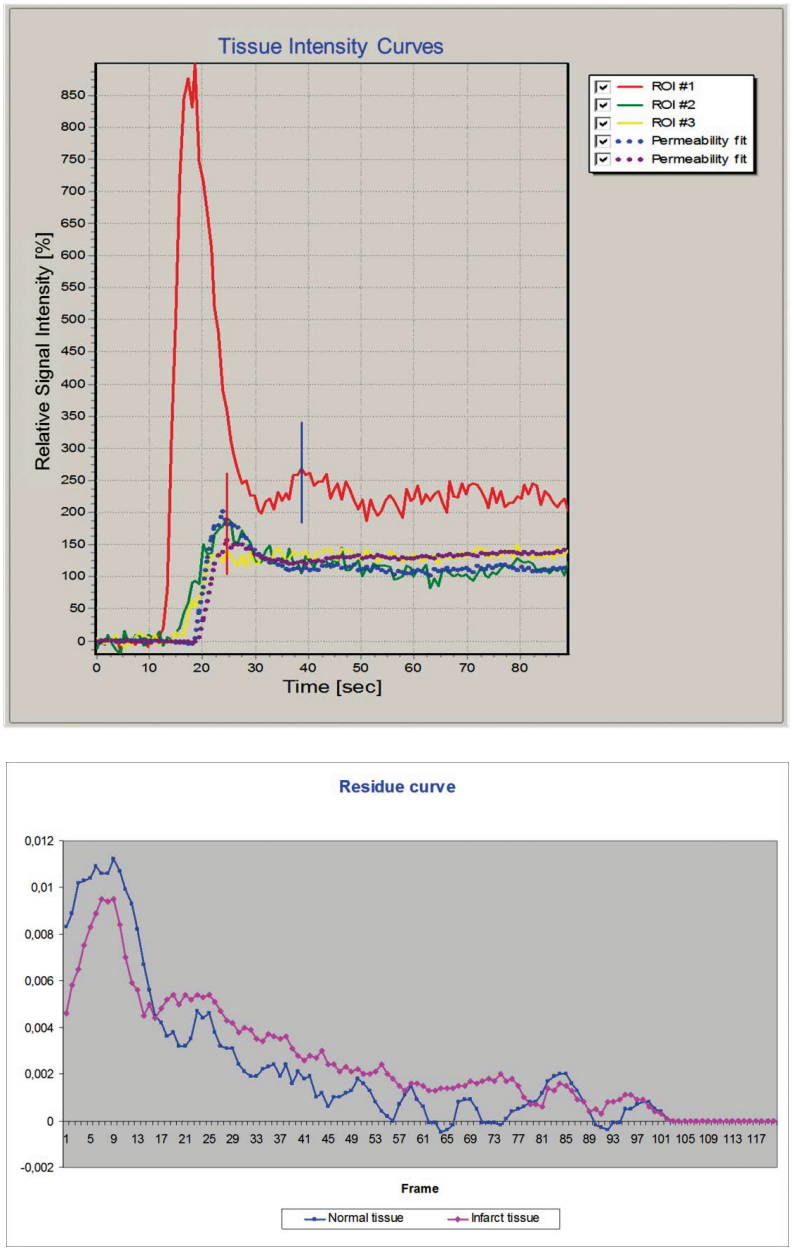

Top: TICs from AIF (red), normal tissue (green) and infarct tissue (yellow), respectively. Blue and purple dotted curves represent fitted curves after deconvolution to AIF.Bottom: Two residue curves of normal (blue) and infarct tissue (purple) from AIF deconvolution

The deconvolution process is mathematically unstable, and different approaches have been introduced to calculate the residue curve in a stable manner[113]. Additional mathematical modeling is needed to eliminate the fact that tissue tracer also has contributions from tracer recirculation. Any realistic modification of the two-compartment model including added tissue compartments makes modeling more complex. The model's dependency on a proportional relationship between contrast concentration and signal intensity is crucial. True quantification is dependent on some correction method in order to avoid T2* effects of the AIF, for instance sufficiently low contrast agent dosage.

1.5.3.3 Assessment of microvascular obstruction

Originally, MO detection with MRI was described as stable hypoenhancement in the infarct zone after first pass perfusion, 1 – 2 min after contrast agent injection[28;120]. Diagnosis depends on T1 imaging at a time point in advance of LGE imaging. However, non-enhancing areas of the infarct core detected at LGE are similarly considered areas of infarct without reperfusion, and have been called severe, late or persistent MO[32;38;121]. Thus, separation into MO and persistent MO is possible, provided that early enhancement and LGE imaging is performed[31;33]. A potential source of error was revealed in an experimental model with part of an acute infarct completely unperfused. This part may still be hyperintense on LGE imaging, if signal intensity of the sequence chosen is dependent on the amplitude of the magnetization vector[122].

1.5.4 Late gadolinium enhancement

Until the late 1990s infarct characterization with MRI was dependent on the precise characterization of regional function. In 1999 Kim et al. utilized the fact that acute and chronic infarcts retain extravascular, extracellular contrast media to a larger extent than viable myocardium does, irrespective of whether the cells are ischemic or not. Infarct delineation between MRI and stained tissue slices correlated remarkably[123]. The main advantage of the new strategy was the ability to differentiate infarcted myocardium from hypokinetic tissue due to reversible ischemia. The breakthrough was facilitated by the introduction of two practical working methods. Infarct imaging was started at least 5 min after contrast agent injection and an inversion recovery sequence provided maximum T1 contrast. The method has gained

widespread use and different terms have been introduced, such as “late enhancement” (LE), “delayed enhancement” (DE), “delayed hyper-enhancement” (DHE) and late gadolinium enhancement (LGE); the latter term is used in this thesis.

Immediately after myocardial infarct, cell membranes of the necrotic cardiomyocytes disintegrate. Later necrotic tissue is replaced by granulation tissue and subsequently by scar tissue with collagen deposits in the extracellular matrix[124]. In all these stages of infarction disease the distribution volume of extravascular, extracellular molecules is increased, causing increased tissue concentration of extracellular contrast agents, and thus shortened T1. Five minutes after a bolus injection of contrast agent steady state has occurred with a stable contrast agent ratio between tissue and plasma[115], and imaging is preferably initiated 10 minutes after contrast agent injection. Maximum T1 contrast is facilitated by the initial inversion recovery pulse, with an inversion time chosen to null viable myocardium which therefore appears dark, whereas non-viable cardiac tissue appears bright. Sequential adjustment of inversion time is recommended due to renal clearance of contrast agent and gradually increasing T1[120;125].

The detection of any focal area with increased extracellular volume is in itself unspecific. A diversity of cardiac pathologies includes the positive finding of LGE, but pattern of LGE and clinical picture vary[126]. The subendocardial to transmural LGE distributed in distinct coronary perfusion areas is highly specific for ischemic heart disease, and according to the Consensus Panel Report of 2004 LGE was considered a first line imaging method in the assessment of myocardial viability and the characterization of acute and chronic myocardial infarction[127].

The extent of infarct affection is of great interest after an acute infarct, and in the preoperative assessment before coronary revascularization. Infarcts may more or less affect the complete myocardial wall, and this depth of infarct from the endocardial border is called transmural affection. Transmurality is closely related to infarct size and prognosis, and has been found to correlate independently with remodeling and function[38]. The presence of a thin subepicardial non-enhancing wall is not sufficient to obtain increased function after revascularization. One study defined a threshold of 75 % transmurality a possible cut-off value for recovery after coronary artery reperfusion in chronic ischemic disease [42]. On the other hand, other studies have

found a threshold of 50 % more convenient; as releated to likelihood for recovery in AMI or after bypass surgery[127].

1.5.5 Cardiac magnetic resonance imaging challenges

Some inherent methodological sources of error apply for almost all cardiac MRI. They occur even under optimal conditions, and some are common for all dynamic cardiac imaging. Probably it is fair to emphasize that in spite of the sources of error below, MRI has a well documented potential for systematic, reproducible and non-subjective reporting of the heart and the heart's movements.

Depending on level of inhalation during a breath-hold, heart position will vary more or less in all three standard axes from one acquisition to another. An apico-basal or *LV axis translation* between acquisitions may result, causing the undetected repetition or omission of one or more slices during the serial short axis imaging of the ventricular complex.

For short axis cine and tagging sequences the tissue at diastole is not completely similar to the tissue at systole, due to the heart's LV axis translation during contraction and relaxation. The error is larger for the basal slices.

With some pulse sequences, there may be a delay of 30-50 ms from the R-wave to acquisition of the first image. Furthermore, with prospective ECG trigging, the last image is acquired with a time margin until next R-wave to compensate for variations in the R-R interval. Thus cine and tagging sequences may *miss part of the end diastolic phase*.

Abrupt contour changes or signal variation of less than the complete slice thickness may be masked or blurred[123]. This *partial-volume effect* is present in all cross-sectional slice imaging, but increases with slice thickness and may be amplified by LV axis translation.

With the exception of ultra-fast acquisition techniques which may allow real-time imaging, one cardiac pulse sequence typically encompasses 6 to 10 heart cycles. The *combination of cycles* makes cardiac MRI prone to motion artifacts, especially in arrhythmia.

1.6 Two-dimensional speckle tracking echocardiography

Echocardiography is ultrasound examination of the heart. Pulses of ultrasound are transmitted into the tissues, and images are based on the reflected echoes. Reflections occur whenever there is a change in acoustic impedance, which is the product of tissue density and ultrasound propagation speed. Speckles are complex grayscale variations, mainly resulting from multiple reflections and the interference from these due to microscopic change in tissue structure. For most diagnostic ultrasound they are considered noise distorting fine details of anatomy[128]. The speckles form an acoustic pattern which is visible in the grayscale image or can be read directly from the received RF signal. For myocardial tissue, this pattern is considered unique for small units of tissue volume, like a finger print. Thus, a small tissue volume or area can be re-identified from image frame to image frame. Computerized identification and tracking of the specific speckles form the base for the characterization of tissue motion with this method.

Common 2D grayscale echocardiography of the heart in standardized image planes are utilized for the application of two-dimensional speckle tracking echocardiography (2D-STE). Quality of tracking is dependent on several factors, like the sufficient delineation of the myocardial wall and endo- and epicardial borders, the avoidance of reverberation artifacts and an adequate frame rate for the tracking of either grayscale or RF speckles. Speckles may change, disappear due to translation from the image plane, or deform. Generally, motion tracking is noisy, and some regularization filtering is applied, in order to secure a logical interpretation.

Tracking of speckles gives information of velocity, direction and deformation as a result of velocity differences between speckles. Thus, motion can be decomposed upon one of the preferred directions and characterized by in-plane strain rate or ε. The technique is independent from insonation angle and with sufficient computer capacity it is quick.

On this background, when 2D-STE was introduced, hope was that the method was able to characterize regional deformation of the LV, as expressed in ε or strain rate, perhaps with even better performance than traditional echocardiographic methods.

2 Aims

In the broader perspective the aim of this thesis was to illustrate the potential for MRI as a research tool in myocardial infarction.

2.1 Specific aims

The aim of paper I was to explore whether intracoronary injection of autologous mononuclear bone marrow cells (mBMC) after AMI influenced regional myocardial function or twist. Further, we aimed to explore the potentials for tagging analysis to detect more subtle changes in myocardial function than those detected by more routinely used examination techniques.

In paper II, the aims were to follow the semi-quantitative parameters from comprehensive analyses of contrast-enhanced myocardial perfusion imaging of infarct tissue, longitudinally from subacute to chronic phase. Furthermore we aimed to correlate the semi-quantitative measurements of subacute infarct tissue to more qualitative enhancement analyses from both perfusion imaging and LGE.

In paper III, we hypothesized that peak systolic longitudinal strain (ε_L) measured by 2D-STE provided additional information regarding the extent of infarct mass and myocardial function when compared with the LVEF and WMSI in patients with chronic myocardial infarct. LGE was used as a reference method for determination of the infarct extent.

3 Material and Methods

3.1 Patients and controls

Paper I and paper II were based on the ASTAMI study which was a prospective, open-labeled, randomized trial. The study was designed with a power of 80 % to identify a potential difference of 5 % points in the development of LVEF between the treatment group and the control group, as measured by single-photon-emission computed tomography. A cohort of patients with ST-segment elevation acute myocardial infarction (STEMI) admitted for acute PCI at Rikshospitalet University Hospital and Ullevål University Hospital were screened for inclusion in the study 1 – 4 days after PCI. After acceptance, 101 patients were randomized by a permuted block randomization stratified according to study center to either treatment with intracoronary injection of mBMC or control. Block size was 4, randomization was 1:1. For the treatment group, mBMC injection was performed 4 – 8 days (mean 6 days) after PCI. The combined procedure of bone marrow aspiration and intracoronary injection of placebo medium was considered unethical, thus controls received no intracoronary sham injection. One patient was later excluded due to heart transplantation. At 6 months all were alive, and no patient was lost in the follow-up. Also see the publication for the trial's main end points for details of inclusion[14].

The MRI examination was performed 2 – 3 weeks after the acute infarction in order to avoid the effect of acute edema, and repeated at 6 months after the insult. At 6 months there were 87 complete pairs of MRI examinations. All MRI examinations included cine imaging, contrast enhanced perfusion at rest and LGE. Midway in the ASTAMI study, the MR unit went through a hardware and software upgrade. bSSFP method for cine imaging was introduced, and the perfusion sequence had been changed with altered dynamic range.

At the end of the trial myocardial tagging was included in the protocol. In paper I 28 patients were included with a protocol of tagging MRI, cine imaging and LGE.

In paper II, 63 patients with paired perfusion MRI either before (n = 39) or after upgrade (n = 24) were included. Before upgrade the perfusion sequence was unstable and aborted early after AIF second pass peak during the run of 6 patients at baseline and 3 at 6 months. In these, only first-pass descriptive enhancement parameters were

measured. Three additional perfusion examinations were lost for qualitative first pass enhancement and MO assessment at baseline due to image noise. One patient refused the final contrast agent injection at 6 months and was excluded for LGE analysis. Thus 54 patients were included for all analyses. Most patients from paper I were also included in paper II.

Paper III was designed as a cross-sectional study of 38 patients included after an index STEMI, treated by PCI. None of the patients were in cardiogenic shock. MRI and echocardiography was performed at follow up, 9.2 ± 5.7 months after PCI. In addition, 15 healthy volunteers of the age 46 ± 12 years (6 female) were included for echocardiography examination. See Table 1 for the comparison of patient characteristics in paper I – III.

All studies comply with the Declaration of Helsinki. The protocols were approved by the regional committee for research ethics. All subjects gave written, informed consent.

Table 1: Characteristics of patients included in paper I - III

	Paper I	Paper II	Paper III
Patient number (female)	28 (6)	63 (9)	38 (10)
Intracoronary mBMC	15	30	-
Age (years)	59 ± 9	57 ± 9	55 ± 10
LVEF (%)	52 ± 10	55 ± 12	58 ± 11
LV EDV (ml)	176 ± 50	166 ± 43	157 ± 53
Infarct size (%)	24 ± 13	22 ± 14	20 ± 13
Anterior wall infarct	28	63	33
Inferior wall infarct	1	-	6
Lateral wall infarct	2	-	3
Peak CK MB (µg/l)	361 ± 136	322 ± 137	301 ± 188

In paper I and II characteristics of study patients at baseline; in paper III LV volumes, infarct size and infarct location from follow-up MRI.

3.2 Imaging methods

All MRI pulse sequences were acquired in the same image session with 1.5 tesla units (Magnetom Vision Plus or Magnetom Sonata, Siemens Healthcare, Erlangen,

Germany) using a phased array body coil. The different imaging modalities, analyses and outcome parameters are referred in Table 2.

Echocardiographic examinations were performed with either a Vivid 5 scanner (seven examinations) or a Vivid 7 scanner (46 examinations) (GE Healthcare Vingmed Ultrasound AS, Horten, Norway), using a phased-array transducer.

Table 2: Imaging and outcome parameters of papers I – III

Modality	Analysis	Outcome parameter	Paper I	Paper II	Paper III
Cine MRI	Biplane	LVEF	X		X
Echocardiography	Area biplane	LVEF			X
	Visual assessment	WMS, WMSI			X
Tagging MRI	HARP software	ε_c, twist	X		
2D-STE	EchoPac software	ε_L, PSSI, early stretch			X
Perfusion MRI	TICs	enhancement parameters		X	
	Deconvolution	K^{trans}, k_{ep}, v_e		X	
	Residue curve	rBF		X	
Perfusion MRI and LGE	Visual assessment	enhancement groups		X	
LGE	Manual contours	infarct size	X	X	X

The different modalities, analysis methods and outcome parameters of paper I - III. LVEF: Left ventricular ejection fraction, WMS and WMSI: wall motion score (index), HARP: Harmonic Phase Imaging, ε_C: circumferential strain, ε_L: longitudinal strain, PSSI: post-systolic shortening index, 2D-STE: two-dimensional speckle tracking echocardiography, TIC: time intensity curve, K^{trans}: the transfer constant, k_{ep}: the rate constant, v_e: volume fraction of extravascular, extracellular tissue, rBF: parameter resembling blood flow from the residue curve, LGE: late gadolinium enhancement.

MRI cine imaging was performed to quantify LV volumes in papers I and III. Tagging MRI was performed in paper I for the assessment of regional ε_C and global LV twist. Perfusion MRI was performed in paper II with the measurement of a spectrum of descriptive enhancement and kinetic parameters, and visual assessment

of perfusion images together with LGE was performed for enhancement grouping. Echocardiography was performed for paper III. From grayscale echocardiography LV volumes and regional WMS and global WMSI were assessed. Additionally 2D grayscale images were analyzed with speckle tracking for ε_L, early stretch and post-systolic shortening index (PSSI). For all papers regional and global infarct size was assessed with LGE. See papers I – III for more detailed method description.

3.3 Blinding of readers and variability assessment

All MRI analysis of the ASTAMI study was performed by readers blinded to treatment allocation.

For paper III, analyses of grayscale echocardiography, speckle tracking and MRI were performed independently by three different observers, blinded to the other results.

Inter- and intraobserver variability assessment of LVEF from cine MRI was performed for the ASTAMI study.

In paper I, ε_C and twist inter- and intra-observer reproducibility was assessed through repeated analyses of 10 randomly selected tagging examinations. Reproducibility of analyses was assessed with two-way mixed absolute agreement intraclass correlation analyses of global and regional ε_C and twist.

In paper II, the MO classification was performed by two independent observers, and decided by consent when disagreement occurred.

In paper III, echocardiography examinations were performed repeatedly by two independent observers on ten randomly selected patients. Repeated echocardiography was assessed with reliability analyses of ε_L values.

3.4 Statistical analyses

Continuous data are presented as mean ± standard deviation (SD).

In paper I, development of treatment groups between 2-3 weeks and 6 months was assessed by analysis of covariance, with the baseline values used as a covariate.

In paper II, paired samples t-tests were performed for the comparison of parameters of normal myocardium versus infarct tissue at baseline and for infarct intra-group

changes. Kruskal-Wallis test was performed to assess differences across the four enhancement groups. If difference was significant, follow up Mann-Whitney U test was performed for difference between pairs of groups with Bonferroni adjustment of the alpha level to 0.008.

In paper III differences between myocardial tissue infarct categories were analyzed with one-way analysis of variance. Bonferroni correction was applied for post-hoc tests and for multiple regression analyses. Values were compared for correlation by regression analysis using a least squares method. A multivariate regression analysis was performed to find the best determinant of the global ε_L. Receiver operating characteristic (ROC) curves were constructed, and AUCs were measured to determine cut-off values for optimal sensitivity and specificity. The ROC analyses were set to identify infarcts of ≥ 30 g at the global level, an infarct size that has been shown to predict poor prognosis[28], infarct size ≥ 5 g at the territorial level and transmural infarct at the segmental level.

Tests were two-sided, and p-values < 0.05 were considered significant. SPSS software versions 16.0, 18.0 and 14.0, respectively (IBM Corporation, New York, NY, USA) were used.

4 Summary of results

4.1 Paper I

In the control group myocardial function as measured by ε_C improved for the global LV (6 months: -13.1 ± 2.4 % versus 2 – 3 weeks: -11.9 ± 3.4 %, p = 0.014) and for the infarct zone (-11.8 ± 3.0 % versus -9.3 ± 4.1 %, p = 0.001), and significantly more than in the mBMC group (inter-group p = 0.027 for global ε_C, respectively p = 0.009 for infarct zone ε_C). LV infarct mass decreased (35.7 ± 20.4 g versus 45.7 ± 29.5 g, p = 0.024), also significantly more pronounced than in the mBMC group (inter-group p = 0.034). LV twist was initially low and remained unchanged irrespective of therapy.

Mean intraclass correlation coefficient (ICC) of agreement for inter-observer judgments was 0.97 (with 95 % confidence interval 0.87 - 0.99), 0.96 (0.83 - 0.99) and 0.95 (0.65 - 0.99) for global, infarct zone and transmural infarct zone ε_C, respectively, and corresponding values for intra-observer observations were 0.99 (0.95 - 1.00), 0.98 (0.81 - 0.99) and 0.96 (0.82 - 0.99). For individual segments agreement was lower with an ICC of 0.81 (0.75 - 0.86) for intra-observer and 0.87 (0.83 - 0.91) for inter-observer judgments. For twist analysis the ICC of agreement for inter-observer judgments was 0.92 (0.74 - 0.98) and 0.96 (0.85 - 0.99) for intra-observer observations.

4.2 Paper II

DCE MRI at rest was performed in 63 patients in the subacute and chronic phase after reperfused myocardial infarct. Initial upslope, enhancement at TTP_n, rBF and k_{ep} were lower and TTP, wash-out slope and v_e were higher in infarct tissue ($p < 0.001$ for all analyses). Infarct tissue v_e decreased to 6 months (p = 0.045). At baseline, infarct tissue with persistent MO had even more delayed TTP, lower rBF, K^{trans}, k_{ep} and enhancement at TTP_n and delayed contrast arrival ($p < 0.008$ for pairwise analyses). Higher rank of qualitative enhancement stratification correlated to larger infarcts ($p < 0.001$).

Correlation for MO classification between observers was moderate ($\kappa = 0.5$, $p < 0.001$). Of the 54 patients, classification was decided by consent for 25 individuals.

Of these, 15 were reclassified. Presence of MO changed for 7 individuals. Differences and conclusions of the material were not affected by reclassification.

4.3 Paper III

In a total of 38 patients, LGE cardiac MRI identified transmural infarction in 27 patients, with a mean infarct size of 36 ± 25 g. Peak systolic ε_L correlated to infarct mass at the global level ($r = 0.84$, $p < 0.01$). A ε_L cut-off value of -15 % identified infarction with 83 % sensitivity and 93 % specificity at the global level, and 76 % and 95 % at the territorial level. A ε_L cut-off value of -13 % identified infarction with 80 % sensitivity and 83 % specificity at the segmental level. Global infarct mass also correlated to wall motion score index ($r = 0.70$, $p < 0.01$), and to LVEF by cardiac MRI or echocardiography ($r = -0.71$ and -0.58, respectively; both $p < 0.01$). Assessment of early stretch and PSSI did not provide additional information by multivariate regression analysis.

Reliability analyses of ε_L revealed a Cronbach's α of 0.90 for inter-observer, and 0.95 for intra-observer variation at the global level, 0.92 and 0.97 at the territorial level and 0.81 and 0.92 at the segmental level.

5 Discussion

5.1 Myocardial infarct

5.1.1 Paper I

Results from paper I did not support any favorable outcome for patients treated with mBMC injection after myocardial infarct. This was a confirmation of earlier findings; primary endpoints from the ASTAMI trial, an exercise study and a three years outcome study all had similar development for the two treatment groups[129-131].

Nevertheless, subtle differences were found. Infarct size as assessed with LGE and ε_C as assessed with tagging MRI developed beneficially for the control group. The first finding was in contrast to the main study, in which infarct size development did not differ between the two groups. Additionally, ε_C development differed from studies on regional function on the complete ASTAMI population as performed with echocardiography[132]. Correlation between ε_C and LGE was confirmed. A substudy on transmurally infarcted segments was performed for comparison with the results of Herbots et al.[133], but our results did not confirm their finding of a more beneficial mBMC effect in this group.

Thus, we did not conclude that the developmental difference between treatment groups was relevant for the complete population of the ASTAMI study. One possible explanation was influence from a non-significant difference in infarct size between treatment groups at baseline MRI. Even though infarct size reduction is larger the first week after the acute incident, some volume reduction is expected at a later stage[134;135], and functional development correlates strongly to LGE. Myocardial edema was not assessed, and this factor could act as an undetected confounder.

More important, our findings confirmed a potential for regional and summarized regional analyses to detect subtle differences in development not found by global LV analysis, as assessed by biplane LVEF with cine MRI in this paper. Since development of methods for regional movement imaging and analysis by MRI, the method has shown a potential for the detailed characterization of wall movement disorders of various origin[136-139], and recently, different developmental ε_C for infarcts with or without edema and hemorrhage has been revealed[140].

The measurements of LV twist revealed low values for the basal/apical rotational movement. Without healthy controls for comparison, we considered the measured values of infarcted ventricles to be in accordance with other studies with reduced LV twist after myocardial infarct. Reduced twist or apical torsion has been considered a sensitive and fast method for the diagnosis of myocardial tissue disease[141], but there are different findings whether reduced torsion regains after infarct. Our interval measurements were stable. However, the examined group of patients was small, and mean LVEF was not severely reduced compared to other studies. Difference may be revealed with larger study group and/or larger population diversity.

5.1.2 Paper II

Perfusion assessment of paper II was comprehensive, with semi-quantitative measurement of descriptive enhancement and kinetic parameters combined with qualitative analyses. We sampled a spectrum of analyses of tissue parameters in order to describe a variety of circulatory features of infarct tissue. Figure 4 repeats a simplified scheme illustrating the relationship between the dynamic enhancement parameters and the kinetic parameters.

From the semi-quantitative parameters we largely confirmed the well-known decrease of perfusion in infarct tissue compared to non-infarcted tissue[142-144]. This decrease characterizes both subacute and chronic infarcts, and is apparent in visual analyses as well, with first pass hypoenhancement for most of the infarcts. Infarct tissue hypoenhancement was stable over the time interval, leading to the conclusion that scar tissue is hypoperfused during first pass compared to myocardium.

K^{trans} was not significantly changed in infarct tissue. This finding was in contrast to an earlier report[145], possibly resulting from setup differences with reperfused infarcts examined subacutely and not acutely. K^{trans} is closely related to flow (F) and the PS product. Thus, an independent flow measurement was needed and rBF was calculated from the residue curve. As suggested in paper II, the explanation for K^{trans} and rBF developing differently could be an increase of the PS product in subacute infarct tissue. Another possibility is masked difference of K^{trans} (as a type II fault), due to variability. Refined studies with more precise quantification and a sufficient

study population at relevant intervals may even better characterize tissue changes and mechanisms of repair over time after myocardial infarct.

Figure 4: Relationship between enhancement and kinetic parameters

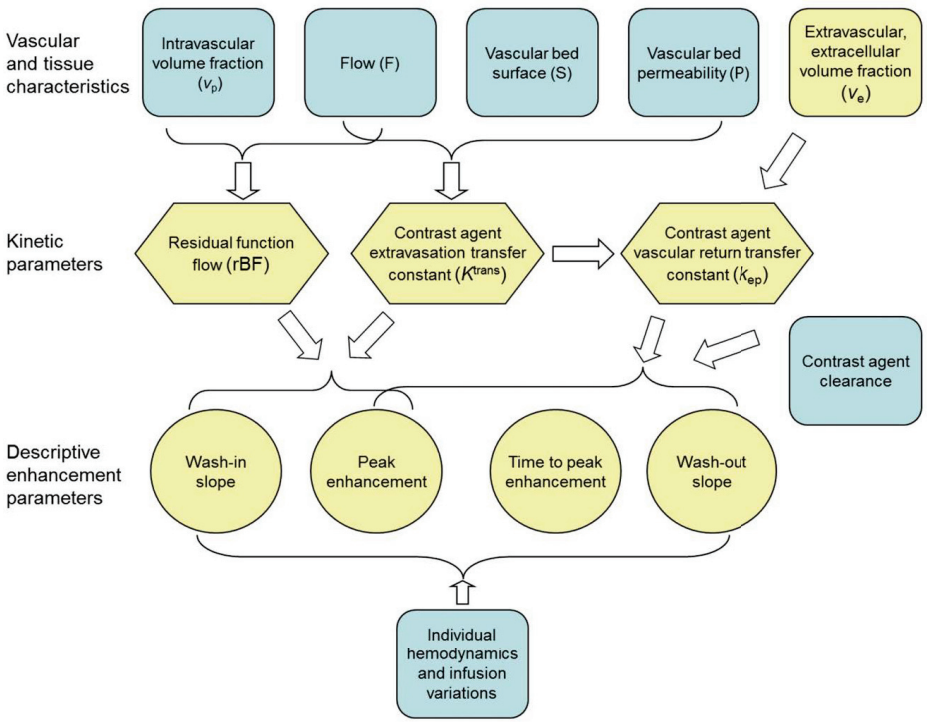

Simplified scheme of the relationship between tissue characteristics, descriptive enhancement parameters and kinetic parameters. Arrows illustrate influence. Yellow figures illustrate parameters directly measured or calculated in paper II.

Qualitative and semi-quantitative analyses were combined, and the relative calculation of enhancement and kinetic parameters revealed added information on microvascular changes of the damaged myocardium. Infarct tissue in individuals with persistent MO had an even more pronounced decrease of perfusion compared to infarcted tissue with lower enhancement score. The study in paper III was not designed to detect whether there was a continuity of flow degradation in infarct tissue, with the central core MO at the extreme, or whether there might be a defined cut-off level of reduced flow at MO. Time point for diagnosing MO was probably not ideal[29;33], and the ROI sampling of tissue was large, compared to the small areas of MO in the infarct.

Furthermore, contrast agent arrival was delayed in the persistent MO group. Based on an experimental animal study, we explained delayed arrival with the possibility for collateral flow[146], although a component of microvessel stenosis was also possible. In the experimental animal study, epicardial arteries were gradually occluded, stimulating collateral circulation from distant coronary territories. In paper II, pathological mechanisms are believed to originate on the microvascular level in the no-reflow territory. More detailed studies at relevant time intervals on the microvasculatory situation are needed to characterize these mechanisms.

5.1.3 Paper III

The main outcome of paper III was the good correlation between detailed regional echocardiography and infarct size and transmurality. ε_L as assessed with 2D-STE was achieved from 90 % of all segments from longitudinal grayscale echocardiography. When defining cut-off levels, severly reduced ε_L identified transmurally infarcted segments, severely infarcted coronary territories, or LVs with large infarcts. The global index of ε_L seemed to perform better for sensitivity and specificity, with the highest AUC of the ROC-analyses. Two possible explanations to the latter are the potentially favorable effect from averaging of noise, and independency from anatomical assignment differences across modalities when global indices are calculated. Visual assessment leading to WMSI similarly detected severe infarction. This finding both confirmed the strong relationship between infarct affection and myocardial function in this population, and the possible strength for regional wall motion analyses in the detailed characterization of the infarcted LV.

Two other parameters, PSSI and early stretch were calculated from 2D-STE. Of these, correlation with infarct size was higher for PSSI. This parameter is virtually different from systolic ε_L, characterizing another mechanical property of diseased myocardium. Two mechanisms can explain the shortening of infarct tissue after end systole; an active but impaired sarcomer shortening in cardiomyocytes, or passive recoil which shortens tissue when wall tension falls. The last mechanism is to a larger extent believed to be present in scar tissue[147]. The ability of PSSI to identify large and transmural infarct in this population gave no clue to the distinction between these two mechanisms, but confirmed presence of the phenomenon. Furthermore, it indicated that quality of 2D-STE was preserved during diastole.

From multivariate analysis we found that global ε_L correlated independently with infarct size, but not with LVEF. This was an interesting finding, considering the relation between global ε_L and LVEF; both characterizing LV contraction. In this paper, the different diagnostic tests were not directly compared against each other with any superiority or non-inferiority test. A later publication revealed better performance for global ε_L than LVEF as examined by echocardiography in the identification of different infarct sizes, and better performance for global ε_L than WMSI in the identification of small and medium-sized infarcts[148].

For the ROC analyses infarct areas were categorized into transmural/not transmural, or large/not large in order to construct dichotomous variables and to quantify sensitivity and specificity. In turn, this led to the definition of cut-off levels for significant pathology of ε_L as measured by 2D-STE. Where to set cut-off levels for the definition of pathology is dependent on the clinical setting. We studied a predefined population, with high incidence of pathology. The important part in this setting was to avoid overlooking decreased myocardial function and large infarcts, thus sensitivity was more important than specificity. Still, the results illuminate a challenge in the definition of a normal level. Non-infarcted tissue in the diseased group had lower ε_L than myocardial tissue in healthy controls. The cut-off value chosen identified large infarcts, and for this purpose also remote tissue of patients was included among normal myocardium. This may not always be the best solution; concerning the possibility that remote remodeling affects clinical parameters of interest in other settings.

5.2 Patient selection

In the present work, all the investigated patients had STEMI treated by PCI. All were between 40 and 75 years old and most had evidence of anterior wall infarct. In paper III, the patient group was more heterogeneous with some patients with lateral and inferior wall infarcts. However, the patient groups were relatively similar regarding age, lower representation of women, mean infarct size and cardiac function (Table 1).

The use of MRI in itself introduces a potential for skewed recruitment of patients to research. First, no incompatible devices are allowed; including several monitoring

devices for critically ill patients, LV assisting devices, and most ICDs and pacemakers. Second, cardiovascular monitoring is challenging in the MR suite, and unstable patients may worsen hemodynamically solely from the laying still on the back through a complete examination. Third, there are still substantial challenges when examining the heart of patients with complex arrhythmia. Forth, the use of Gd is precluded in patients with seriously decreased renal function, although the relationship between nephrogenic systemic fibrosis and Gd was unknown at the time of patient inclusion for these three studies.

Care must therefore be taken to generalize findings from these studies.

5.3 Study design

5.3.1 Paper I

As a substudy of the larger ASTAMI study, paper I was an open-labeled, randomized prospective study. The main aim was similar to the aim of the ASTAMI trial; effect from treatment with intracoronary injection of mBMC, for this paper assessed with the secondary endpoints ε_C and LV twist. The ASTAMI study in itself was designed to have sufficient power to detect a difference of 5 % points of LVEF as examined by single-photon-emission computed tomography. For paper I power was assumed inferior because of low inclusion number.

Reduced inclusion compared to the main ASTAMI study was caused by the shortened inclusion time interval. Characteristics of sub populations may be different from the total population due to sample error, but no known systematic error had been introduced. The distribution between treatment and control was quite even, and there was no significant difference in baseline characteristics between treatment groups.

5.3.2 Paper II

Although another substudy of the ASTAMI study, design and purpose of paper II differed. The objects studied were infarct tissue versus non-infarcted myocardium, with an interval study on infarct tissue. Treatment groups with or without intracoronary mBMC injection were merged, and the interventional aspect of the

ASTAMI study was not taken into account. Thus, this paper is a prospective, comparative observational study.

Merge of the 2 treatment groups was based on the presumption that neither infarcted nor non-infarcted myocardial tissue differed between the groups. This was supported by earlier reports from the ASTAMI study[129-132;149]. All perfusion and enhancement parameters were controlled for treatment effect without detecting difference, and all correlation analyses were performed with treatment randomization as covariate without any correlation or influence on other correlation. We concluded that the presumption was justified.

5.3.3 Paper III

The purpose of this study was the exploration of different non-invasive diagnostic tests for the assessment of LV function. A cross-sectional design was considered adequate.

Diagnostic methods are often tested without the knowledge of the true value of the parameter to be measured. Infarct size characterized with LGE served the role as reference method; no gold standard for regional LV function was chosen. We believed chronic myocardial infarct to be the sole explanation of myocardial function reduction. This assumption was indirectly, but only partly controlled for by the LGE assessment[126].

ROC-curves of the diagnostic tests and correlation between LGE and the different test methods were considered suitable graphical summaries to illustrate the performance of diagnostic tests[150]. Difference between test scores was not explored, and this study was not designed to conclude that any of the diagnostic tests were superior or inferior to the others[151].

5.4 Reliability

Reliability refers to parameter consistency, depending on precision and accuracy.

5.4.1 Infarct detection and extent

For all studies, the correct diagnosis of infarct size, transmurality and location with LGE was crucial. In paper I infarct size was one of the endpoints reported, and the segments were subgrouped according to transmurality classification. In paper II the

interpretation of infarct and non-infarct tissue decided ROI placement for infarct and non-infarct TIC calculation. Infarct size was an important covariate, and LGE was even important in the qualitative assessment of enhancement groups. In paper III segmental, territorial and global infarct size and infarct percent were the reference measurements for the diagnostic tools to be tested.

Method for LGE performance and image analysis has proven robust[152], and standard procedures were well proven and according to international guidelines. Contrast agent dosage recommendations vary between 0.1 – 0.2 mmol Gd/kg[120;125;152]. For the higher dosage, one has to wait sufficiently long after contrast agent injection before imaging in order to avoid masking of subendocardial high intensity due to high blood pool intensity[125]. Inversion time has to be adjusted to null normal myocardium signal intensity, irrespective of dosage and time point after contrast agent injection.

Short axis views covering the complete LV were utilized for manual LGE delineation. When infarct border was dubious, cross-correlation to long axis images was performed. When still in doubt a cut-off value of neighboring myocardium signal intensity + 2 SD for infarct tissue was utilized, as reported in paper III. This may look controversial, when regarding a recommendation of + 5 SD as a threshold, concluding that + 2 SD was associated with overestimation of effective infarct size[153]. In this respect, it is important to notice that the recommendation was valid for automated quantification software. To date, choice of threshold level is still not established[120;152]. Infarcts of relatively lower intensity do exist [154]. For paper I - III manual analysis was performed. This is still regarded the most precise method, and for such the threshold is of less controversy[120]. In our experience, local signal intensity difference between viable and infarcted tissue is far exceeding the + 2 SD threshold, also confirmed by an early report on LGE imaging and analysis[42].

Infarct transmurality is directly derived from infarct size assessment; dependent on the reading of LGE imaging with a precise anatomical assignment. We defined transmurality level based on percent scar. However, definition of transmurally infarcted segments differed two of the papers; ≥ 75 % in paper I and ≥ 50 % in paper III. In paper I the threshold of 75 % was chosen in order to compare results to the publication by Herbots et al.[133]. This threshold has been shown to be of clinical

interest[42]. The threshold of 50 % in paper III was similar to earlier publications exploring regional ε and strain rate after myocardial infarct[155;156].

Infarct assessment in these studies relied on a well-proven method, the correct delineation of hyperenhancing myocardium and robust anatomical assignment also corresponding to anatomical assignment of the other imaging methods. For these studies, infarct tissue was examined in the subacute and chronic stages. Infarct tissue was clearly hyperenhancing, and earlier phase infarct assessment would have brought more confounding edema. Correlation to regional function was excellent.

5.4.2 Left ventricular volumes and ejection fraction

LV volumes, as assessed by cine MRI for paper I and III were calculated from two long axis projections using the "biplane ellipsoid formula". At the time for study design; this method was regarded fast and sufficiently accurate for volume measurements[90;92;93]. The formula is based on the understanding of the LV as a regular 3D ellipsoid, each axis with different radius. Volume is derived from the equation

$$V = \frac{8 \cdot A_1 \cdot A_2}{3\pi \cdot l} \tag{6}$$

where A_1 and A_2 are the areas of the ventricular cavity in each long axis projection, and l is the LV long axis. The main objections to the formula are the principal objection to the presumption of a symmetric 3D object, secondarily that the model lacks adjustment for irregular contraction, and third the fact that the cut end at the base is not taken into account.

Later studies and general recommendations have stressed the increased accuracy and decreased variability of the application of Simpson's rule with the summing of a complete set of short axis slices[157] although for clinical purposes a fast evaluation with the biplane technique may be considered acceptable[120].

Change from spoiled GRE to bSSFP cine in our institution affected cine sequences of papers I and III. Measurements were known to vary between these two acquisitions[83;84]. Care was taken to secure that all patients of the ASTAMI study were examined with paired either spoiled GRE or bSSFP, this was relevant for paper

I. In paper III, both methods were represented in the study population. Inter- and intraobserver variability assessment of the ASTAMI study revealed that variability for spoiled GRE acquisition was larger than for bSSFP (Figure 5)[158]. Even though variability assessment was performed only from a random sample among all ASTAMI patients, the calculations were performed in the same period of time, and we believe the numbers to be relevant for the examinations of paper I and III.

Figure 5: Inter-observer variability assessment for the ASTAMI study

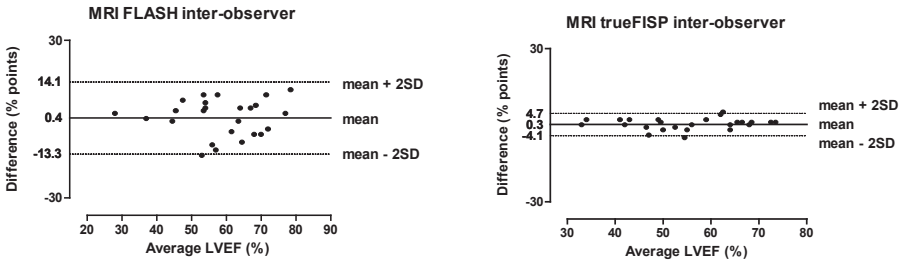

Bland Altman plots from inter-observer variability assessment for LVEF in the ASTAMI study Left: spoiled GRE sequence (FLASH), right: bSSFP (trueFISP)

The method chosen for volume calculation and the observed variability may have masked differences between groups in paper I or diminished precision in paper III.

5.4.3 Strain and torsion

In papers I and III good correlation between regional ε and LGE was confirmed. However, ε is known to be load dependent, and this may be part of the explanation for decreased ε in remote areas after infarct[159-161]. In these papers, all patients were hemodynamically stable, and results are not believed to be severely influenced from individual variation of load.

5.4.3.1 Tagging MRI

For HARP analysis of tagging MRI, inter- and intra-observer assessment has been performed as a part of the large Multi-Ethnic Study of Atherosclerosis[108]. As in paper I, agreement was good. The authors reported that mid-wall ε_C was more stable, with best agreement for peak ε_C. Identifiable tag fading made diastolic analysis less stable. As stated above, the CSPAMM technique enables more stable tags; this has

later been utilized by a study on the early post-systolic phase after myocardial infarct[162].

Software HARP version 1.0 was used for analysis. Mid-wall Lagrangian ε_C was calculated from the deformation curves in 24 points in each slice. The software version was semi-automatic with limited ability for the correction of erroneous tracking ("tag jumping"). Thus, tag noise prolonged analysis time and caused extreme ε_C values of some single points. This was managed with the exclusion of ε_C values > 10 % and < -30 %. Figure 6 illustrates systolic tag jumping of one registration point, and ε_C curves before and after exclusion. Most often tag jumping led to elongation of the deformation line. Thus, noise mainly reduces ε_C amplitude, partially corrected by exclusion. More complex noise involving several neighboring points led to exclusion of segments, and even territories.

Torsion analyses seemed more robust. Data were less characterized by noise, and no exclusion was performed. Torsion analysis agreement was good. No control group was examined. In paper I absolute torsion measurement in infarcted hearts were lower than in normal hearts reported in other studies, and were considered reduced[163;164]. We were not able to confirm any longitudinal alteration of decreased torsion after infarction in paper I.

Tagging results revealed ε_C differences in the study population. The differences correlated well with infarct size and infarct size development. Sample size was small, and noise led to exclusions. However, agreement was good, and thus, results were considered reliable.

Figure 6: Tag jumping and exclusion of extreme values

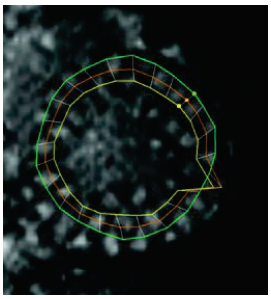

End systolic (7^{th}) frame (left) from Harp analysis of a mid-ventricular slice without LGE. Note tag jumping of one point, causing elongation of two deformation lines with the resulting positive ε_C of the anterolateral segment (middle). ε_C curves (bottom) after exclusion of two extreme values.

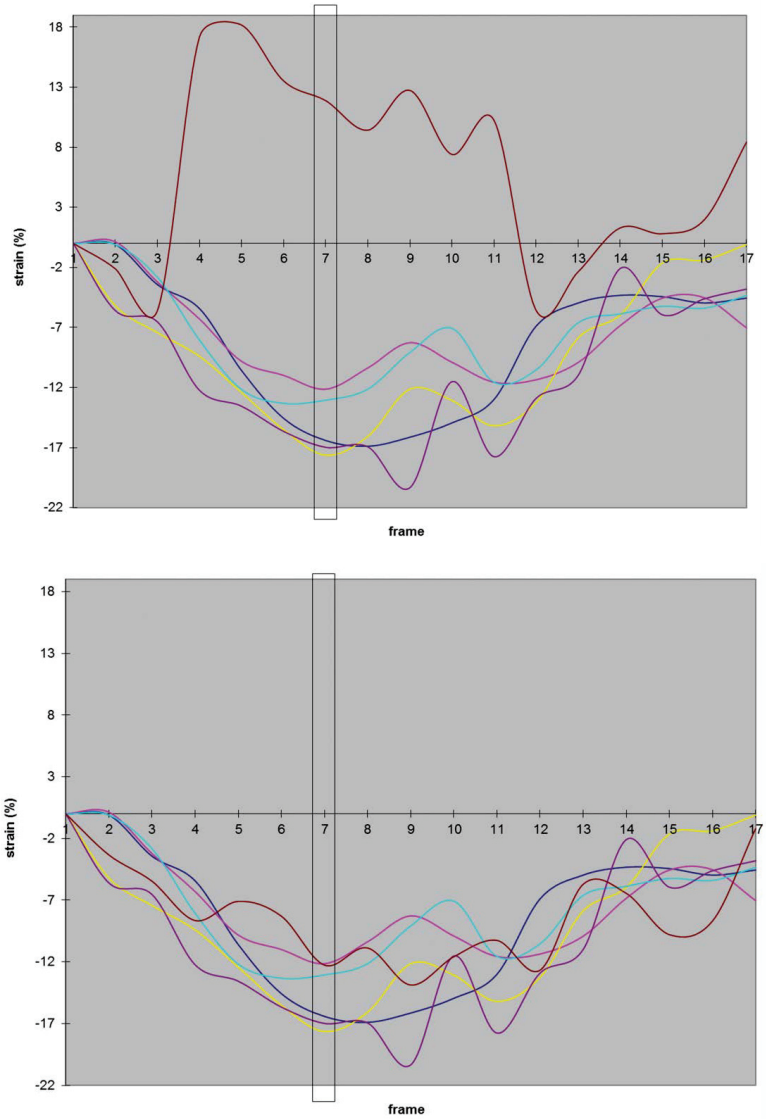

5.4.3.2 Two-dimensional speckle tracking echocardiography

Proper 2D-STE registration is dependent on quality echocardiography with good delineation of myocardium, lack of reverberations and a sufficient frame rate. For paper III, 90 % of all LV segments were included for ε_L analysis, and variability assessment from repeated echocardiography showed good correlation for ε_L assessment. In other studies, variability between observers has varied between moderate and good[163;164], though in one study reproducibility for ε_L scored even better than tagging MRI[165].

For paper III ε_L, PSSI and early stretch were examined on the segment level, territorial level and global LV level. Performance for the identification of severe infarct was better for global examination, probably as a result from noise averaging and independence from anatomical assignment. We have seen even better correlation to segmental infarct affection in a recent 3D area ε study, and part of this improvement may be the easier anatomical assignment[166]. The territorial indices may seem artificial, considering the large inter-individual variation in coronary perfusion territories. However, for clinical purposes this assessment is relevant with the potential not only to diagnose typical infarct distribution, but also to discriminate severe from less severe infarct affection. The averaging of global ε_L is logical, providing a parameter for the global LV function. The averaging of PSSI in fact provided a parameter with almost similar potential for severe infarct identification. Early stretch was a less sensitive marker of severe infarct affection in paper III.

The main impact of paper III was the illustration of reliability of ε_L as a parameter with potential for the assessment of severe regional myocardial affection. Although noise may be a challenge, and some exclusion was made, scores were good especially on the global level, with good correlation for repeated echocardiography examination. This is in accordance with later studies, which have confirmed good performance of ε_L as assessed by 2D-STE[167-170]. A recent study has even indicated superior performance of ε_L compared to more conventional echocardiographic methods[171].

5.4.4 Myocardial perfusion

Absolute perfusion quantification by MRI has been correlated to labeled blood cells or injected microspheres in animal models [158;172-174] and with human positron emission tomography studies[118;175;176]. Correlation is moderate to good, and methodological refinement is probably needed. An inter-study approach revealed a coefficient of variation > 25 % for myocardial perfusion measurement at stress[177]. The absolute perfusion quantification is among other details dependent on a reliable measurement of the arterial input and an appropriate mathematical model for the deconvolution of tissue intensity measurements to the input function.

The main challenge for a reliable AIF measurement is the non-linearity between signal intensity and contrast agent concentration[178;179]. Different contrast agent infusion regimes have been tested, including the infusion of smaller dosage. Contrast agent dosage has to be < 0.03 mmol Gd/kg if not to exceed non-linearity between AIF and contrast concentration of more than 10 – 15 %. Underestimation of arterial contrast agent concentration will in turn cause overestimation of tissue perfusion.

The process of deconvolution is very sensitive to noisy data, introducing a risk for large resulting differences[180]. Different modeling has been tested to obtain physiological solutions to the calculations, among which the model independent analysis seems to the most stable[181].

Enhancement parameters directly measured from TICs are not dependent on modeling, and some parameters are closely related to flow. However, these parameters vary with hemodynamic and infusion variations[182]. Normalizing against the AIF stabilizes this variation, but for some of the parameters the non-linearity of the AIF becomes a challenge. In paper II, we believe the variation to be partially controlled by standardized infusion regimes in hemodynamically stable patients. An attempt to normalize tissue enhancement parameters to AIF did not reduce variability.

The combination with visual assessment of perfusion sequences demanded a sufficiently high contrast agent dosage, and absolute perfusion measurement was precluded due to T2* effects. Thus, we presented relative and semi-quantitative measurements. Quality of data was reduced by the unforeseen alteration of perfusion

sequence due to magnet upgrade. Table 3 lists some different parameters before and after upgrade.

Table 3: Perfusion sequence parameters before and after MR unit upgrade

	Flip angle	TE	TI	Spatial resolution	Slice thickness	Stacks	Temporal resolution
Before upgrade	88°	1.2 ms	300 ms	1.17 mm	10 mm	60	2 heart beats
After upgrade	158°	0.96 ms	100 ms	1.36 – 1.52 mm	8 mm	120	1 heart beat

TE: echo time, TI: inversion time

Among these parameters, an inversion time of 300 ms might be longer than desired[183]. Shortening the inversion time reduces the non-linearity T2* effect, but signal to noise ratio may be reduced. The alteration of this parameter may have changed the dynamic range of the perfusion sequence. In order to correct for this error, only paired examinations either before or after upgrade were included. Patients examined with different perfusion sequences at the two time points were excluded from the material, reducing sample size and possibly power. For correlation analyses, perfusion sequence was included as a covariate parameter.

Paired comparison was performed between infarct and normal tissue. Possibly the term remote tissue would have been more appropriate. Reduced contractile function in remote myocardium after AMI has been shown, explained by dilatation and/or loading conditions[138;161;184]. The early changes in remote myocardium after AMI are not completely understood, and a recent study not only revealed reduced contraction, but also T1 shortening in remote myocardium, additionally coupled to the finding of deposition of fibrous tissue and possibly inflammatory mechanisms[185]. Reduced perfusion has not been considered part of changes of remote myocardium. On the other hand, any alteration of extracellular matrix should influence wash-out, k_{ep} and v_e.

Interval examination of infarct tissue confirmed presence of reduced perfusion and increased v_e in chronic infarct tissue, as compared to normal myocardium. Over time, v_e decreased without change of other perfusion parameters. This was in accordance

with studies on infarct tissue with estimation of the myocardial tissue-blood partition coefficient[124;186], whereas longitudinal studies on perfusion are scarce. In normal subjects and even in a group of subjects with coronary disease, inter study variability of DCE MRI has been measured to be in the magnitude of variability of perfusion studies with positron emission tomography[187-189]. Physiological variation, measurement variation and variation from calculation may be present, and the implication of longitudinal differences is not completely assessed[190].

To sum up, the quantification of perfusion in this study was semi-quantitative and measurement levels cannot be directly compared to results from other studies. Several design challenges exist, but altogether, the main consequence was probably masking of difference. The measured differences between infarcted and non-infarcted tissue are believed to be reliable.

5.4.5 Microvascular obstruction

The qualitative assessment of infarct tissue enhancement was performed as a combined analysis of early phase perfusion imaging and LGE. Such qualitative assessment is prone to subjectivity. In order to ensure reliability, clear criteria for identifying MO were defined. Analysis was performed by two independent observers, and for disagreement qualitative enhancement grouping was settled by consent. This procedure proved necessary with moderate correlation between observers.

As stated above both subacute infarct and scar tissue are generally hypoperfused during first pass compared to non-infarcted myocardium. This was confirmed for a great majority of the infarcts with relative hypoenhancement subacutely, as an ordinary finding after myocardial infarct. Measurements revealed substantial differences between enhancement groups, with a more severe perfusion reduction in tissue with persistent MO than with first pass hypoenhancement only. Qualitative visualization of the difference is probably dependent on a series of technical parameters including sequence parameters, in-plane resolution and contrast agent dosage. However, the finding emphasizes the difference between first pass hypoperfusion and MO, and the term MO should be reserved for infarct tissue with a

hypoenhancing zone at a later stage after contrast agent infusion than at first pass[28;120].

Our observations led us to believe there is continuity between MO and persistent MO. The area of persistent MO was invariably a lesser part of the MO area; but on the other hand the finding of MO did not always lead to a finding of persistent MO. This is consistent with previous descriptions of persistent MO[31;33]. Although the natural time course for MO is not clarified, we suspect there is a similar temporal continuity, with the final resolution of the central core MO occurring from days to weeks after the acute incident. In paper III we did not correlate MO to prognostic factors. The different enhancement groups were small and adverse events were scarce. Presence of MO and size of the present MO correlate to infarct size, and in some studies MO has shown independent impact on prognosis[28;31-33]. One serial study suggested a correlation between later resolution of the central core MO and adverse remodelling[33]. However, the complete relation between MO and prognosis remains to be clarified; whether MO size, classification to MO or persistent MO, time point for MO resolution or the independent contribution from infarct size are most important.

Correlation between enhancement groups and semi-quantitative measurements were not influenced by re-grouping after consent between observers. Thus, findings were considered reliable. The comprehensive analyses emphasized the need for more studies on early and late microvasculatory changes of acute infarct.

5.5 Validity

The goal in myocardial infarct research is to reduce mortality and morbidity of the disease. Consequently, the relevant primary endpoints for this research are death, reinfarction and symptoms from cardiac disease. However, such research is in the need for large sample sizes and long follow-up, associated with high cost and risk for missing data and noncompliance. Medical imaging and other diagnostic tests therefore may provide surrogate endpoints, in order to overcome these shortcomings; at least partially. Surrogate endpoints are biomarkers of disease, expected to predict clinical benefit or harm. Advantages of surrogate endpoints are the potential for studies with smaller sample size, shorter follow-up and to a larger extent restriction

to one center trials. This is caused by the endpoint variable to reflect biological changes with lower threshold than the primary endpoints. Biomarkers can play the role as surrogate endpoints provided they are reliable and valid.

For a biomarker to be valid, change of the biomarker has to be relevant for outcome. Relationship between morbidity or mortality and the surrogate endpoint has to be biologically plausible. The prognostic value for the surrogate has to be demonstrated in epidemiological studies. And finally, there has to be evidence that treatment effect influencing the surrogate corresponds to clinically relevant effects[191]. Even though validity is plausible, evidence lacks for this last point for many parameters.

LVEF is a valid surrogate endpoint. Infarct size assessed with LGE is reliable, and is believed valid, although the proving for treatment effect on LGE to influence clinical relevant effects still lacks. Assessment of regional dysfunction is sensitive and has proven reliable. However, validity for minor differences not detectable with traditional global assessment is until now more questionable. For perfusion imaging MO is thought to be a valid parameter, but the complete assessment of reliability is missing[191].

A recent meta-analysis on surrogate studies versus primary endpoint studies, found a difference between the two groups. Trials reporting surrogate endpoint were more likely to report larger treatment effects than the other group of trials reporting final patient relevant outcomes[192]. Probably this partly reflects the main advantages of surrogate endpoints as sensitive parameters in research. Nevertheless, effects on surrogate endpoints have to be considered with caution.

6 Conclusions

6.1 Paper I

LGE and ε_C quite similarly demonstrate subtle differences between the mBMC and control groups. No beneficial regional or global effect on myocardial function is detected after mBMC injection.

6.2 Paper II

Reperfused infarct tissue has reduced perfusion and increased v_e compared to normal tissue, and infarct tissue v_e decreases with scarring. The presence of persistent MO results in delayed contrast arrival time and an even more pronounced perfusion reduction.

6.3 Paper III

Peak systolic ε_L by 2D-STE correlates to the infarct mass assessed by LGE at a global level, and separates infarcted from non-infarcted tissue. ε_L is an excellent predictor of myocardial infarct size and transmurality in chronic ischemic heart disease.

6.4 Conclusion of the Thesis

MRI is a valuable tool for the detection of subtle, regional differences in myocardial infarct tissue. Comprehensive MRI combining relevant pulse sequences has potential to illuminate complex patophysiological mechanisms. Cardiac MRI may be used as reference for the validation of new diagnostic tests characterizing the infarcted heart.

7 Future perspectives

Dynamic MRI is a powerful diagnostic tool for myocardial infarction, and carries valuable surrogate endpoints for research on ischemic heart disease. Speckle tracking echocardiography may have similar power in the assessment of myocardial function.

LV volumes and LVEF as assessed with MRI are reliable and valid surrogate endpoints for further interventional cardiac research. Regional and global function assessed with either echocardiography or MRI has the potential for even more precise characterization of the LV. When proven valid, this improved characterization may refine clinical research. Infarct assessment with LGE is another reliable surrogate endpoint for cardiac research, although complete consensus for image analysis is still missing[120].

There is considerable challenge concerning the absolute quantification of myocardial perfusion MRI. Positron emission tomography is the current gold standard for flow measurement in the myocardium, and further validation and refinement of the method is needed. Method for the assessment of MO may still develop, in order to come closer to consensus for contrast agent administration and time after injection for ideal read-out. Additionally, more knowledge about the natural course of MO is needed[191].

Since the publication of paper I - III, technical evolution and refinement of methods have continued. New methods have been introduced, reliability has for some been confirmed. T2 imaging may have a role in assessment of AMI for salvage examination[193;194]. T1 mapping has been introduced and seems to have great potential in the characterization of diseased myocardium, and cardiac proton spectroscopy has entered the field of clinical research[185;195]. However, there is still need to make evidence for a majority of the tools as reliable and valid surrogate endpoints for trials[191]. These new applications already here provide potentials for more detailed assessment of myocardial infarct disease as to increase understanding of necrosis, reperfusion, microvascular damage and repair. MRI and echo combined with other modalities through hybrid solutions and image fusion are other perspectives for comprehensive research and increased understanding[122;185;195].

At last, we have to keep in mind that surrogate endpoints are not primary.

8 References

1 World Health Organization. Global burden of coronary heart disease. 2011. http://www.who.int/cardiovascular_diseases/en/cvd_atlas_13_coronaryHD.pdf accessed: 28-6-2013.

2 World Health Organization. Deaths from coronary heart disease. 2011. http://www.who.int/cardiovascular_diseases/en/cvd_atlas_14_deathHD.pdf accessed: 28-6-2013.

3 World Health Organization. Milestones in knowledge of heart and vascular disorders: 1969-2004. 2011. http://www.who.int/cardiovascular_diseases/en/cvd_atlas_28_MILS_1969_2004.pdf accessed: 28-6-2013.

4 Pfeffer MA, Braunwald E. Ventricular remodeling after myocardial infarction. Experimental observations and clinical implications. *Circulation* 1990; **81**(4):1161-1172.

5 Fishbein MC, Maclean D, Maroko PR. The histopathologic evolution of myocardial infarction. *Chest* 1978; **73**(6):843-849.

6 Braunwald E, Pfeffer MA. Ventricular enlargement and remodeling following acute myocardial infarction: mechanisms and management. *Am J Cardiol* 1991; **68**(14):1D-6D.

7 Jackson KA, Majka SM, Wang H, Pocius J, Hartley CJ, Majesky MW, Entman ML, Michael LH, Hirschi KK, Goodell MA. Regeneration of ischemic cardiac muscle and vascular endothelium by adult stem cells. *J Clin Invest* 2001; **107**(11):1395-1402.

8 Orlic D, Kajstura J, Chimenti S, Jakoniuk I, Anderson SM, Li B, Pickel J, McKay R, Nadal-Ginard B, Bodine DM, Leri A, Anversa P. Bone marrow cells regenerate infarcted myocardium. *Nature* 2001; **410**(6829):701-705.

9 Britten MB, Abolmaali ND, Assmus B, Lehmann R, Honold J, Schmitt J, Vogl TJ, Martin H, Schachinger V, Dimmeler S, Zeiher AM. Infarct remodeling after intracoronary progenitor cell treatment in patients with acute myocardial infarction (TOPCARE-AMI): mechanistic insights from serial contrast-enhanced magnetic resonance imaging. *Circulation* 2003; **108**(18):2212-2218.

10 Wollert KC, Meyer GP, Lotz J, Ringes-Lichtenberg S, Lippolt P, Breidenbach C, Fichtner S, Korte T, Hornig B, Messinger D, Arseniev L, Hertenstein B, Ganser A, Drexler H. Intracoronary autologous bone-marrow cell transfer after myocardial infarction: the BOOST randomised controlled clinical trial. *Lancet* 2004; **364**(9429):141-148.

11 Janssens S, Dubois C, Bogaert J, Theunissen K, Deroose C, Desmet W, Kalantzi M, Herbots L, Sinnaeve P, Dens J, Maertens J, Rademakers F, Dymarkowski S, Gheysens O, Van CJ, Bormans G, Nuyts J, Belmans A, Mortelmans L, Boogaerts M, Van de WF. Autologous bone marrow-derived stem-cell transfer in patients with ST-segment elevation myocardial infarction: double-blind, randomised controlled trial. *Lancet* 2006; **367**(9505):113-121.

12 Hirsch A, Nijveldt R, van d, V, Biemond BJ, Doevendans PA, van Rossum AC, Tijssen JG, Zijlstra F, Piek JJ. Intracoronary infusion of autologous mononuclear bone marrow cells or peripheral mononuclear blood cells after primary percutaneous coronary intervention: rationale and design of the HEBE trial--a prospective, multicenter, randomized trial. *Am Heart J* 2006; **152**(3):434-441.

13 Schachinger V, Tonn T, Dimmeler S, Zeiher AM. Bone-marrow-derived progenitor cell therapy in need of proof of concept: design of the REPAIR-AMI trial. *Nat Clin Pract Cardiovasc Med* 2006; **3 Suppl 1**:S23-S28.

14 Lunde K, Solheim S, Aakhus S, Arnesen H, Abdelnoor M, Forfang K. Autologous stem cell transplantation in acute myocardial infarction: The ASTAMI randomized controlled trial. Intracoronary transplantation of autologous mononuclear bone marrow cells, study design and safety aspects. *Scand Cardiovasc J* 2005; **39**(3):150-158.

15 Sanz G, Castaner A, Betriu A, Magrina J, Roig E, Coll S, Pare JC, Navarro-Lopez F. Determinants of prognosis in survivors of myocardial infarction: a prospective clinical angiographic study. *N Engl J Med* 1982; **306**(18):1065-1070.

16 de Albuquerque CP, Kalil-Filho R, Gerstenblith G, Nakano O, Barbosa V, Bellotti G, Pileggi F, Tranchesi B. Long-term function in the remote region after myocardial infarction: importance of significant coronary stenoses in the non-infarct-related artery. *Br Heart J* 1994; **71**(3):249-253.

17 Cerqueira MD, Weissman NJ, Dilsizian V, Jacobs AK, Kaul S, Laskey WK, Pennell DJ, Rumberger JA, Ryan T, Verani MS. Standardized myocardial segmentation and nomenclature for tomographic imaging of the heart: a statement for healthcare professionals from the Cardiac Imaging Committee of the Council on Clinical Cardiology of the American Heart Association. *Circulation* 2002; **105**(4):539-542.

18 Shiina A, Tajik AJ, Smith HC, Lengyel M, Seward JB. Prognostic significance of regional wall motion abnormality in patients with prior myocardial infarction: a prospective correlative study of two-dimensional echocardiography and angiography. *Mayo Clin Proc* 1986; **61**(4):254-262.

19 Schiller NB, Shah PM, Crawford M, DeMaria A, Devereux R, Feigenbaum H, Gutgesell H, Reichek N, Sahn D, Schnittger I, . Recommendations for quantitation of the left ventricle by two-dimensional echocardiography. American Society of Echocardiography Committee on Standards, Subcommittee on Quantitation of Two-Dimensional Echocardiograms. *J Am Soc Echocardiogr* 1989; **2**(5):358-367.

20 Mirsky I, Parmley WW. Assessment of passive elastic stiffness for isolated heart muscle and the intact heart. *Circ Res* 1973; **33**(2):233-243.

21 Edvardsen T, Urheim S, Skulstad H, Steine K, Ihlen H, Smiseth OA. Quantification of left ventricular systolic function by tissue Doppler echocardiography: added value of measuring pre- and postejection velocities in ischemic myocardium. *Circulation* 2002; **105**(17):2071-2077.

22 Coghlan C, Hoffman J. Leonardo da Vinci's flights of the mind must continue: cardiac architecture and the fundamental relation of form and function revisited. *Eur J Cardiothorac Surg* 2006; **29 Suppl 1**:S4-17.

23 Opdahl A, Helle-Valle T, Remme EW, Vartdal T, Pettersen E, Lunde K, Edvardsen T, Smiseth OA. Apical rotation by speckle tracking echocardiography: a simplified bedside index of left ventricular twist. *J Am Soc Echocardiogr* 2008; **21**(10):1121-1128.

24 McDonald IG. The shape and movements of the human left ventricle during systole. A study by cineangiography and by cineradiography of epicardial markers. *Am J Cardiol* 1970; **26**(3):221-230.

25 Gjesdal O, Hopp E, Vartdal T, Lunde K, Helle-Valle T, Aakhus S, Smith HJ, Ihlen H, Edvardsen T. Global longitudinal strain measured by two-dimensional speckle tracking echocardiography is closely related to myocardial infarct size in chronic ischaemic heart disease. *Clin Sci (Lond)* 2007; **113**(6):287-296.

26 de Jong MC, Genders TS, van Geuns RJ, Moelker A, Hunink MG. Diagnostic performance of stress myocardial perfusion imaging for coronary artery disease: a systematic review and meta-analysis. *Eur Radiol* 2012; **22**(9):1881-1895.

27 Jaarsma C, Leiner T, Bekkers SC, Crijns HJ, Wildberger JE, Nagel E, Nelemans PJ, Schalla S. Diagnostic performance of noninvasive myocardial perfusion imaging using single-photon emission computed tomography, cardiac magnetic resonance, and positron emission tomography imaging for the detection of obstructive coronary artery disease: a meta-analysis. *J Am Coll Cardiol* 2012; **59**(19):1719-1728.

28 Wu KC, Zerhouni EA, Judd RM, Lugo-Olivieri CH, Barouch LA, Schulman SP, Blumenthal RS, Lima JA. Prognostic significance of microvascular obstruction by magnetic resonance imaging in patients with acute myocardial infarction. *Circulation* 1998; **97**(8):765-772.

29 Rochitte CE, Lima JA, Bluemke DA, Reeder SB, McVeigh ER, Furuta T, Becker LC, Melin JA. Magnitude and time course of microvascular obstruction and tissue injury after acute myocardial infarction. *Circulation* 1998; **98**(10):1006-1014.

30 Kloner RA, Ganote CE, Jennings RB. The "no-reflow" phenomenon after temporary coronary occlusion in the dog. *J Clin Invest* 1974; **54**(6):1496-1508.

31 Cochet AA, Lorgis L, Lalande A, Zeller M, Beer JC, Walker PM, Touzery C, Wolf JE, Brunotte F, Cottin Y. Major prognostic impact of persistent microvascular obstruction as assessed by contrast-enhanced cardiac magnetic resonance in reperfused acute myocardial infarction. *Eur Radiol* 2009; **19**(9):2117-2126.

32 Hombach V, Grebe O, Merkle N, Waldenmaier S, Hoher M, Kochs M, Wohrle J, Kestler HA. Sequelae of acute myocardial infarction regarding cardiac structure and function and their prognostic significance as assessed by magnetic resonance imaging. *Eur Heart J* 2005; **26**(6):549-557.

33 Ørn S, Manhenke C, Greve OJ, Larsen AI, Bonarjee VV, Edvardsen T, Dickstein K. Microvascular obstruction is a major determinant of infarct healing and subsequent left ventricular remodelling following primary percutaneous coronary intervention. *Eur Heart J* 2009; **30**(16):1978-1985.

34 Gerber BL, Rochitte CE, Melin JA, McVeigh ER, Bluemke DA, Wu KC, Becker LC, Lima JA. Microvascular obstruction and left ventricular remodeling early after acute myocardial infarction. *Circulation* 2000; **101**(23):2734-2741.

35 Wu KC, Kim RJ, Bluemke DA, Rochitte CE, Zerhouni EA, Becker LC, Lima JA. Quantification and time course of microvascular obstruction by contrast-enhanced echocardiography and magnetic resonance imaging following acute myocardial infarction and reperfusion. *J Am Coll Cardiol* 1998; **32**(6):1756-1764.

36 Lund GK, Stork A, Saeed M, Bansmann MP, Gerken JH, Muller V, Mester J, Higgins CB, Adam G, Meinertz T. Acute myocardial infarction: evaluation with first-pass enhancement and delayed enhancement MR imaging compared with 201Tl SPECT imaging. *Radiology* 2004; **232**(1):49-57.

37 Bogaert J, Kalantzi M, Rademakers FE, Dymarkowski S, Janssens S. Determinants and impact of microvascular obstruction in successfully reperfused ST-segment elevation myocardial infarction. Assessment by magnetic resonance imaging. *Eur Radiol* 2007; **17**(10):2572-2580.

38 Tarantini G, Razzolini R, Cacciavillani L, Bilato C, Sarais C, Corbetti F, Marra MP, Napodano M, Ramondo A, Iliceto S. Influence of transmurality, infarct size, and severe microvascular obstruction on left ventricular remodeling and function after primary coronary angioplasty. *Am J Cardiol* 2006; **98**(8):1033-1040.

39 Kaandorp TA, Lamb HJ, Viergever EP, Poldermans D, Boersma E, van der Wall EE, de RA, Bax JJ. Scar tissue on contrast-enhanced MRI predicts left ventricular remodelling after acute infarction. *Heart* 2007; **93**(3):375-376.

40 Schuijf JD, Kaandorp TA, Lamb HJ, van der Geest RJ, Viergever EP, van der Wall EE, de RA, Bax JJ. Quantification of myocardial infarct size and transmurality by contrast-enhanced magnetic resonance imaging in men. *Am J Cardiol* 2004; **94**(3):284-288.

41 Kachenoura N, Redheuil A, Herment A, Mousseaux E, Frouin F. Robust assessment of the transmural extent of myocardial infarction in late gadolinium-enhanced MRI studies using appropriate angular and circumferential subdivision of the myocardium. *Eur Radiol* 2008; **18**(10):2140-2147.

42 Kim RJ, Wu E, Rafael A, Chen EL, Parker MA, Simonetti O, Klocke FJ, Bonow RO, Judd RM. The use of contrast-enhanced magnetic resonance imaging to identify reversible myocardial dysfunction. *N Engl J Med* 2000; **343**(20):1445-1453.

43 Kolipaka A, Chatzimavroudis GP, White RD, Lieber ML, Setser RM. Relationship between the extent of non-viable myocardium and regional left ventricular function in chronic ischemic heart disease. *J Cardiovasc Magn Reson* 2005; **7**(3):573-579.

44 Lanzer P, Barta C, Botvinick EH, Wiesendanger HU, Modin G, Higgins CB. ECG-synchronized cardiac MR imaging: method and evaluation. *Radiology* 1985; **155**(3):681-686.

45 Ridgway JP. Cardiovascular magnetic resonance physics for clinicians: part I. *J Cardiovasc Magn Reson* 2010; **12**:71.

46 Du YP, Saranathan M, Foo TK. An accurate, robust, and computationally efficient navigator algorithm for measuring diaphragm positions. *J Cardiovasc Magn Reson* 2004; **6**(2):483-490.

47 American Society for Testing and Materials International. American Society for Testing and Materials International. Designation: ASTM F2052 - 06e1, Standard test method for measurement of magnetically induced displacement force on medical devices in the magnetic resonance environment. West Conshohocken,Pa:
2006. http://www.astm.org/Standards/F2052.htm accessed: 28-6-2013.

48 American Society for Testing and Materials International. American Society for Testing and Materials International. Designation: ASTM F2119 - 07 Standard test method for evaluation of MR image artifacts from passive implants. West Conshohocken, PA:
2007. http://www.astm.org/Standards/F2119.htm accessed: 28-6-2013.

49 American Society for Testing and Materials International. American Society for Testing and Materials International. Designation: ASTM F2182 - 11a Standard test method for measurement of radio frequency induced heating on or near passive implants during magnetic resonance imaging. West Conshohocken, PA:
2011. http://www.astm.org/Standards/F2182.htm accessed: 28-6-2013.

50 American Society for Testing and Materials International. American Society for Testing and Materials International. Designation: ASTM F2213 - 06 (2011) Standard test method for measurement of magnetically induced torque on medical devices in the magnetic resonance environment. West Conshohocken, PA: 2011. http://www.astm.org/Standards/F2213.htm accessed: 28-6-0013.

51 U.S.Food and Drug Administration. Guidance for industry and FDA staff: Establishing safety and compatibility of passive implants in the magnetic resonance (MR) environment.
2008. http://www.fda.gov/downloads/MedicalDevices/DeviceRegulationandGuidance/GuidanceDocuments/UCM107708.pdf accessed: 28-6-2013.

52 Shellock FG, Spinazzi A. MRI safety update 2008: part 2, screening patients for MRI. *AJR Am J Roentgenol* 2008; **191**(4):1140-1149.

53 MRI safety, bioeffects and patient management; official website for the institute for magnetic resonance safety, education, and research. 2011. http://www.mrisafety.com/ accessed: 28-6-2013.

54 Hundley WG, Bluemke DA, Finn JP, Flamm SD, Fogel MA, Friedrich MG, Ho VB, Jerosch-Herold M, Kramer CM, Manning WJ, Patel M, Pohost GM, Stillman AE, White RD, Woodard PK. ACCF/ACR/AHA/NASCI/SCMR 2010 expert consensus document on cardiovascular magnetic resonance: a report of the American College of Cardiology Foundation Task Force on Expert Consensus Documents. *Circulation* 2010; **121**(22):2462-2508.

55 Cohen JD, Costa HS, Russo RJ. Determining the risks of magnetic resonance imaging at 1.5 tesla for patients with pacemakers and implantable cardioverter defibrillators. *Am J Cardiol* 2012; **110**(11):1631-1636.

56 Russo RJ. Determining the risks of clinically indicated nonthoracic magnetic resonance imaging at 1.5 T for patients with pacemakers and implantable cardioverter-defibrillators: rationale and design of the MagnaSafe Registry. *Am Heart J* 2013; **165**(3):266-272.

57 Buendía F, Sánchez-Gómez JM, Sancho-Tello MJ, Olagüe J, Osca J, Cano O, Arnau MA, Igual B. Nuclear magnetic resonance imaging in patients with cardiac pacing devices. *Rev Esp Cardiol* 2010; **63**(6):735-739.

58 Wright O. Patient killed by heart blunder. London, UK:
2004. http://www.thetimes.co.uk/tto/news/uk/article1905003.ece accessed: 6-7-2013.

59 Anfinsen OG, Berntsen RF, Aass H, Kongsgaard E, Amlie JP. Implantable cardioverter defibrillator dysfunction during and after magnetic resonance imaging. *Pacing Clin Electrophysiol* 2002; **25**(9):1400-1402.

60 Gimbel JR. Unexpected asystole during 3T magnetic resonance imaging of a pacemaker-dependent patient with a 'modern' pacemaker. *Europace* 2009; **11**(9):1241-1242.

61 Fontaine JM, Mohamed FB, Gottlieb C, Callans DJ, Marchlinski FE. Rapid ventricular pacing in a pacemaker patient undergoing magnetic resonance imaging. *Pacing Clin Electrophysiol* 1998; **21**(6):1336-1339.

62 Cronin EM, Mahon N, Wilkoff BL. MRI in patients with cardiac implantable electronic devices. *Expert Rev Med Devices* 2012; **9**(2):139-146.

63 Wilkoff BL, Bello D, Taborsky M, Vymazal J, Kanal E, Heuer H, Hecking K, Johnson WB, Young W, Ramza B, Akhtar N, Kuepper B, Hunold P, Luechinger R, Puererfellner H, Duru F, Gotte MJ, Sutton R, Sommer T. Magnetic resonance imaging in patients with a pacemaker system designed for the magnetic resonance environment. *Heart Rhythm* 2011; **8**(1):65-73.

64 Colletti PM, Shinbane JS, Shellock FG. "MR-conditional" pacemakers: the radiologist's role in multidisciplinary management. *AJR Am J Roentgenol* 2011; **197**(3):W457-W459.

65 Weigelt JC, Stoltenberg K. St. Jude Medical Announces European Approval of Accent MRI Pacemaker System
New innovative pacing system designed and tested for safe MRI performance. St. Jude Medical; 2011. http://investors.sjm.com/phoenix.zhtml?c=73836&p=irol-newsArticle&ID=1551284 accessed: 6-7-2013.

66 ClinicalTrials.gov. ProMRI Study of the Entovis Pacemaker System.
2013. http://clinicaltrials.gov/ct2/show/NCT01761162 accessed: 6-7-2013.

67 Stomp W. BIOTRONIK ProMRI Pacing Systems Gain European Approval. medgadget; 2010. http://www.medgadget.com/2010/04/biotronik_promri_pacing_systems_gain_european_approval.html accessed: 6-7-2013.

68 Sarvestani A. Biotronik lands Euro approval for MRI-friendly heart implants. Massachusetts Medical Devices Journal LLC; 2013. http://www.massdevice.com/news/biotronik-lands-euro-approval-mri-friendly-heart-implants accessed: 6-7-2013.

69 Hartnell GG, Spence L, Hughes LA, Cohen MC, Saouaf R, Buff B. Safety of MR imaging in patients who have retained metallic materials after cardiac surgery. *AJR Am J Roentgenol* 1997; **168**(5):1157-1159.

70 Cowper SE, Robin HS, Steinberg SM, Su LD, Gupta S, LeBoit PE. Scleromyxoedema-like cutaneous diseases in renal-dialysis patients. *Lancet* 2000; **356**(9234):1000-1001.

71 Kuo PH, Kanal E, bu-Alfa AK, Cowper SE. Gadolinium-based MR contrast agents and nephrogenic systemic fibrosis. *Radiology* 2007; **242**(3):647-649.

72 Grobner T. Gadolinium--a specific trigger for the development of nephrogenic fibrosing dermopathy and nephrogenic systemic fibrosis? *Nephrol Dial Transplant* 2006; **21**(4):1104-1108.

73 Marckmann P, Skov L, Rossen K, Dupont A, Damholt MB, Heaf JG, Thomsen HS. Nephrogenic systemic fibrosis: suspected causative role of gadodiamide used for contrast-enhanced magnetic resonance imaging. *J Am Soc Nephrol* 2006; **17**(9):2359-2362.

74 Chewning RH, Murphy KJ. Gadolinium-based contrast media and the development of nephrogenic systemic fibrosis in patients with renal insufficiency. *J Vasc Interv Radiol* 2007; **18**(3):331-333.

75 Sadowski EA, Bennett LK, Chan MR, Wentland AL, Garrett AL, Garrett RW, Djamali A. Nephrogenic systemic fibrosis: risk factors and incidence estimation. *Radiology* 2007; **243**(1):148-157.

76 Collidge TA, Thomson PC, Mark PB, Traynor JP, Jardine AG, Morris ST, Simpson K, Roditi GH. Gadolinium-enhanced MR imaging and nephrogenic systemic fibrosis: retrospective study of a renal replacement therapy cohort. *Radiology* 2007; **245**(1):168-175.

77 Shellock FG, Spinazzi A. MRI safety update 2008: part 1, MRI contrast agents and nephrogenic systemic fibrosis. *AJR Am J Roentgenol* 2008; **191**(4):1129-1139.

78 Morcos SK. Nephrogenic systemic fibrosis following the administration of extracellular gadolinium based contrast agents: is the stability of the contrast agent molecule an important factor in the pathogenesis of this condition? *Br J Radiol* 2007; **80**(950):73-76.

79 Crownover BK, Bepko JL. Appropriate and safe use of diagnostic imaging. *Am Fam Physician* 2013; **87**(7):494-501.

80 Thomsen HS. ESUR guideline: gadolinium-based contrast media and nephrogenic systemic fibrosis. *Eur Radiol* 2007; **17**(10):2692-2696.

81 European Society of Urogenital Radiology. ESUR guidelines on contrast media 8.0; 1.3.2 Nephrogenic systemic fibrosis (NSF). 2012. http://www.esur.org/guidelines/ accessed: 28-6-2013.

82 The European Medicines Agency (EMEA). Gadolinium-containing contrast agents. 2010. http://www.ema.europa.eu/ema/index.jsp?curl=pages/medicines/human/referrals/Gadoli

nium-containing_contrast_agents/human_referral_000182.jsp&mid=WC0b01ac05805c516f accessed: 28-6-2013.

83 Moon JC, Lorenz CH, Francis JM, Smith GC, Pennell DJ. Breath-hold FLASH and FISP cardiovascular MR imaging: left ventricular volume differences and reproducibility. *Radiology* 2002; **223**(3):789-797.

84 Barkhausen J, Ruehm SG, Goyen M, Buck T, Laub G, Debatin JF. MR evaluation of ventricular function: true fast imaging with steady-state precession versus fast low-angle shot cine MR imaging: feasibility study. *Radiology* 2001; **219**(1):264-269.

85 Semelka RC, Tomei E, Wagner S, Mayo J, Caputo G, O'Sullivan M, Parmley WW, Chatterjee K, Wolfe C, Higgins CB. Interstudy reproducibility of dimensional and functional measurements between cine magnetic resonance studies in the morphologically abnormal left ventricle. *Am Heart J* 1990; **119**(6):1367-1373.

86 Attili AK, Schuster A, Nagel E, Reiber JH, van der Geest RJ. Quantification in cardiac MRI: advances in image acquisition and processing. *Int J Cardiovasc Imaging* 2010; **26 Suppl 1**:27-40.

87 Petitjean C, Dacher JN. A review of segmentation methods in short axis cardiac MR images. *Med Image Anal* 2011; **15**(2):169-184.

88 Dulce MC, Mostbeck GH, Friese KK, Caputo GR, Higgins CB. Quantification of the left ventricular volumes and function with cine MR imaging: comparison of geometric models with three-dimensional data. *Radiology* 1993; **188**(2):371-376.

89 Teichholz LE, Kreulen T, Herman MV, Gorlin R. Problems in echocardiographic volume determinations: echocardiographic-angiographic correlations in the presence of absence of asynergy. *Am J Cardiol* 1976; **37**(1):7-11.

90 Sievers B, Brandts B, Franken U, Trappe HJ. Single and biplane TrueFISP cardiovascular magnetic resonance for rapid evaluation of left ventricular volumes and ejection fraction. *J Cardiovasc Magn Reson* 2004; **6**(3):593-600.

91 Benjelloun H, Cranney GB, Kirk KA, Blackwell GG, Lotan CS, Pohost GM. Interstudy reproducibility of biplane cine nuclear magnetic resonance measurements of left ventricular function. *Am J Cardiol* 1991; **67**(16):1413-1420.

92 Schroeder AP, Houlind K, Pedersen EM, Nielsen TT, Egeblad H. Biplane long-axis magnetic resonance imaging. Survey projections for rapid estimation of left ventricular mass and global function. *Scand Cardiovasc J* 2001; **35**(6):385-393.

93 Lawson MA, Blackwell GG, Davis ND, Roney M, Dell'Italia LJ, Pohost GM. Accuracy of biplane long-axis left ventricular volume determined by cine magnetic resonance imaging in patients with regional and global dysfunction. *Am J Cardiol* 1996; **77**(12):1098-1104.

94 Zerhouni EA, Parish DM, Rogers WJ, Yang A, Shapiro EP. Human heart: tagging with MR imaging--a method for noninvasive assessment of myocardial motion. *Radiology* 1988; **169**(1):59-63.

95 Ibrahim e. Myocardial tagging by Cardiovascular Magnetic Resonance: evolution of techniques--pulse sequences, analysis algorithms, and applications. *J Cardiovasc Magn Reson* 2011; **13**:36.

96 Simpson RM, Keegan J, Firmin DN. MR assessment of regional myocardial mechanics. *J Magn Reson Imaging* 2013; **37**(3):576-599.

97 Fischer SE, McKinnon GC, Maier SE, Boesiger P. Improved myocardial tagging contrast. *Magn Reson Med* 1993; **30**(2):191-200.

98 Pan L, Prince JL, Lima JA, Osman NF. Fast tracking of cardiac motion using 3D-HARP. *IEEE Trans Biomed Eng* 2005; **52**(8):1425-1435.

99 Osman NF, Kerwin WS, McVeigh ER, Prince JL. Cardiac motion tracking using CINE harmonic phase (HARP) magnetic resonance imaging. *Magn Reson Med* 1999; **42**(6):1048-1060.

100 Aletras AH, Ding S, Balaban RS, Wen H. DENSE: displacement encoding with stimulated echoes in cardiac functional MRI. *J Magn Reson* 1999; **137**(1):247-252.

101 Axel L, Dougherty L. MR imaging of motion with spatial modulation of magnetization. *Radiology* 1989; **171**(3):841-845.

102 Axel L, Dougherty L. Heart wall motion: improved method of spatial modulation of magnetization for MR imaging. *Radiology* 1989; **172**(2):349-350.

103 Zhang S, Douglas MA, Yaroslavsky L, Summers RM, Dilsizian V, Fananapazir L, Bacharach SL. A Fourier based algorithm for tracking SPAMM tags in gated magnetic resonance cardiac images. *Med Phys* 1996; **23**(8):1359-1369.

104 Osman NF, McVeigh ER, Prince JL. Imaging heart motion using harmonic phase MRI. *IEEE Trans Med Imaging* 2000; **19**(3):186-202.

105 Osman NF, Prince JL. Visualizing myocardial function using HARP MRI. *Phys Med Biol* 2000; **45**(6):1665-1682.

106 Garot J, Bluemke DA, Osman NF, Rochitte CE, McVeigh ER, Zerhouni EA, Prince JL, Lima JA. Fast determination of regional myocardial strain fields from tagged cardiac images using harmonic phase MRI. *Circulation* 2000; **101**(9):981-988.

107 Rosen BD, Edvardsen T, Lai S, Castillo E, Pan L, Jerosch-Herold M, Sinha S, Kronmal R, Arnett D, Crouse JR, III, Heckbert SR, Bluemke DA, Lima JA. Left ventricular concentric remodeling is associated with decreased global and regional systolic function: the Multi-Ethnic Study of Atherosclerosis. *Circulation* 2005; **112**(7):984-991.

108 Castillo E, Osman NF, Rosen BD, El-Shehaby I, Pan L, Jerosch-Herold M, Lai S, Bluemke DA, Lima JA. Quantitative assessment of regional myocardial function with MR-tagging in a multi-center study: interobserver and intraobserver agreement of fast strain analysis with Harmonic Phase (HARP) MRI. *J Cardiovasc Magn Reson* 2005; **7**(5):783-791.

109 Edvardsen T, Rosen BD, Pan L, Jerosch-Herold M, Lai S, Hundley WG, Sinha S, Kronmal RA, Bluemke DA, Lima JA. Regional diastolic dysfunction in individuals with left ventricular hypertrophy measured by tagged magnetic resonance imaging--the Multi-Ethnic Study of Atherosclerosis (MESA). *Am Heart J* 2006; **151**(1):109-114.

110 Rosen BD, Lima JA, Nasir K, Edvardsen T, Folsom AR, Lai S, Bluemke DA, Jerosch-Herold M. Lower myocardial perfusion reserve is associated with decreased regional left ventricular function in asymptomatic participants of the multi-ethnic study of atherosclerosis. *Circulation* 2006; **114**(4):289-297.

111 Gebker R, Paetsch I, Neuss M, Schnackenburg B, Bornstedt A, Jahnke C, Gomaa O, Fleck E, Nagel E. Determinants of myocardial response in CMR perfusion imaging using Gd-BOPTA (Multihance). *J Cardiovasc Magn Reson* 2005; **7**(3):565-572.

112 Di Bella EV, Parker DL, Sinusas AJ. On the dark rim artifact in dynamic contrast-enhanced MRI myocardial perfusion studies. *Magn Reson Med* 2005; **54**(5):1295-1299.

113 Jerosch-Herold M. Quantification of myocardial perfusion by cardiovascular magnetic resonance. *J Cardiovasc Magn Reson* 2010; **12**:57.

114 Tofts PS, Brix G, Buckley DL, Evelhoch JL, Henderson E, Knopp MV, Larsson HB, Lee TY, Mayr NA, Parker GJ, Port RE, Taylor J, Weisskoff RM. Estimating kinetic parameters from dynamic contrast-enhanced T(1)-weighted MRI of a diffusable tracer: standardized quantities and symbols. *J Magn Reson Imaging* 1999; **10**(3):223-232.

115 Jerosch-Herold M, Sheridan DC, Kushner JD, Nauman D, Burgess D, Dutton D, Alharethi R, Li D, Hershberger RE. Cardiac magnetic resonance imaging of myocardial contrast uptake and blood flow in patients affected with idiopathic or familial dilated cardiomyopathy. *Am J Physiol Heart Circ Physiol* 2008; **295**(3):H1234-H1242.

116 Zierler KL. Equations for measuring blood flow by external monitoring of radioisotopes. *Circ Res* 1965; **16**:309-321.

117 St Lawrence KS, Lee TY. An adiabatic approximation to the tissue homogeneity model for water exchange in the brain: I. Theoretical derivation. *J Cereb Blood Flow Metab* 1998; **18**(12):1365-1377.

118 Jerosch-Herold M, Wilke N, Stillman AE. Magnetic resonance quantification of the myocardial perfusion reserve with a Fermi function model for constrained deconvolution. *Med Phys* 1998; **25**(1):73-84.

119 Kroll K, Wilke N, Jerosch-Herold M, Wang Y, Zhang Y, Bache RJ, Bassingthwaighte JB. Modeling regional myocardial flows from residue functions of an intravascular indicator. *Am J Physiol* 1996; **271**(4 Pt 2):H1643-H1655.

120 Schulz-Menger J, Bluemke DA, Bremerich J, Flamm SD, Fogel MA, Friedrich MG, Kim RJ, von Knobelsdorff-Brenkenhoff F, Kramer CM, Pennell DJ, Plein S, Nagel E. Standardized image interpretation and post processing in cardiovascular magnetic resonance: Society for Cardiovascular Magnetic Resonance (SCMR) Board of Trustees Task Force on Standardized Post Processing. *J Cardiovasc Magn Reson* 2013; **15**(1):35.

121 de WS, Desch S, Eitel I, Fuernau G, Zachrau J, Leuschner A, Gutberlet M, Schuler G, Thiele H. Impact of early vs. late microvascular obstruction assessed by magnetic resonance imaging on long-term outcome after ST-elevation myocardial infarction: a comparison with traditional prognostic markers. *Eur Heart J* 2010; **31**(21):2660-2668.

122 Hedström E, Arheden H, Eriksson R, Johansson L, Ahlstrom H, Bjerner T. Importance of perfusion in myocardial viability studies using delayed contrast-enhanced magnetic resonance imaging. *J Magn Reson Imaging* 2006; **24**(1):77-83.

123 Kim RJ, Fieno DS, Parrish TB, Harris K, Chen EL, Simonetti O, Bundy J, Finn JP, Klocke FJ, Judd RM. Relationship of MRI delayed contrast enhancement to irreversible injury, infarct age, and contractile function. *Circulation* 1999; **100**(19):1992-2002.

124 Arheden H, Saeed M, Higgins CB, Gao DW, Bremerich J, Wyttenbach R, Dae MW, Wendland MF. Measurement of the distribution volume of gadopentetate dimeglumine at echo-planar MR imaging to quantify myocardial infarction: comparison with 99mTc-DTPA autoradiography in rats. *Radiology* 1999; **211**(3):698-708.

125 Kim RJ, Shah DJ, Judd RM. How we perform delayed enhancement imaging. *J Cardiovasc Magn Reson* 2003; **5**(3):505-514.

126 Bogaert J, Dymarkowski S. Delayed contrast-enhanced MRI: use in myocardial viability assessment and other cardiac pathology. *Eur Radiol* 2005; **15 Suppl 2**:B52-B58.

127 Pennell DJ, Sechtem UP, Higgins CB, Manning WJ, Pohost GM, Rademakers FE, van Rossum AC, Shaw LJ, Yucel EK. Clinical indications for cardiovascular magnetic resonance (CMR): Consensus Panel report. *Eur Heart J* 2004; **25**(21):1940-1965.

128 Loupas T, McDicken WN, Allan PL. Noise reduction in ultrasonic images by digital filtering. *Br J Radiol* 1987; **60**(712):389-392.

129 Beitnes JO, Hopp E, Lunde K, Solheim S, Arnesen H, Brinchmann JE, Forfang K, Aakhus S. Long-term results after intracoronary injection of autologous mononuclear bone marrow cells in acute myocardial infarction: the ASTAMI randomised, controlled study. *Heart* 2009; **95**(24):1983-1989.

130 Lunde K, Solheim S, Aakhus S, Arnesen H, Abdelnoor M, Egeland T, Endresen K, Ilebekk A, Mangschau A, Fjeld JG, Smith HJ, Taraldsrud E, Grøgaard HK, Bjørnerheim R, Brekke M, Muller C, Hopp E, Ragnarsson A, Brinchmann JE, Forfang K. Intracoronary injection of mononuclear bone marrow cells in acute myocardial infarction. *N Engl J Med* 2006; **355**(12):1199-1209.

131 Lunde K, Solheim S, Aakhus S, Arnesen H, Moum T, Abdelnoor M, Egeland T, Endresen K, Ilebekk A, Mangschau A, Forfang K. Exercise capacity and quality of life after intracoronary injection of autologous mononuclear bone marrow cells in acute myocardial infarction: results from the Autologous Stem cell Transplantation in Acute Myocardial Infarction (ASTAMI) randomized controlled trial. *Am Heart J* 2007; **154**(4):710-718.

132 Beitnes JO, Gjesdal O, Lunde K, Solheim S, Edvardsen T, Arnesen H, Forfang K, Aakhus S. Left ventricular systolic and diastolic function improve after acute myocardial infarction treated with acute percutaneous coronary intervention, but are not influenced by intracoronary injection of autologous mononuclear bone marrow cells: a 3 year serial echocardiographic sub-study of the randomized-controlled ASTAMI study. *Eur J Echocardiogr* 2011; **12**(2):98-106.

133 Herbots L, D'hooge J, Eroglu E, Thijs D, Ganame J, Claus P, Dubois C, Theunissen K, Bogaert J, Dens J, Kalantzi M, Dymarkowski S, Bijnens B, Belmans A, Boogaerts M, Sutherland G, Van de WF, Rademakers F, Janssens S. Improved regional function after autologous bone marrow-derived stem cell transfer in patients with acute myocardial infarction: a randomized, double-blind strain rate imaging study. *Eur Heart J* 2009; **30**(6):662-670.

134 Engblom H, Hedstrom E, Heiberg E, Wagner GS, Pahlm O, Arheden H. Rapid initial reduction of hyperenhanced myocardium after reperfused first myocardial infarction suggests recovery of the peri-infarction zone: one-year follow-up by MRI. *Circ Cardiovasc Imaging* 2009; **2**(1):47-55.

135 Ibrahim T, Hackl T, Nekolla SG, Breuer M, Feldmair M, Schomig A, Schwaiger M. Acute myocardial infarction: serial cardiac MR imaging shows a decrease in delayed enhancement of the myocardium during the 1st week after reperfusion. *Radiology* 2010; **254**(1):88-97.

136 Götte MJ, Germans T, Russel IK, Zwanenburg JJ, Marcus JT, van Rossum AC, van Veldhuisen DJ. Myocardial strain and torsion quantified by cardiovascular magnetic resonance tissue tagging: studies in normal and impaired left ventricular function. *J Am Coll Cardiol* 2006; **48**(10):2002-2011.

137 Edvardsen T, Gerber BL, Garot J, Bluemke DA, Lima JA, Smiseth OA. Quantitative assessment of intrinsic regional myocardial deformation by Doppler strain rate

echocardiography in humans: validation against three-dimensional tagged magnetic resonance imaging. *Circulation* 2002; **106**(1):50-56.

138 Götte MJ, van Rossum AC, Twisk JWR, Kuijer JPA, Marcus JT, Visser CA. Quantification of regional contractile function after infarction: strain analysis superior to wall thickening analysis in discriminating infarct from remote myocardium. *J Am Coll Cardiol* 2001; **37**(3):808-817.

139 Marcus JT, Götte MJ, van Rossum AC, Kuijer JP, Heethaar RM, Axel L, Visser CA. Myocardial function in infarcted and remote regions early after infarction in man: assessment by magnetic resonance tagging and strain analysis. *Magn Reson Med* 1997; **38**(5):803-810.

140 Kidambi A, Mather AN, Motwani M, Swoboda P, Uddin A, Greenwood JP, Plein S. The effect of microvascular obstruction and intramyocardial hemorrhage on contractile recovery in reperfused myocardial infarction: insights from cardiovascular magnetic resonance. *J Cardiovasc Magn Reson* 2013; **15**(1):58.

141 Opdahl A, Helle-Valle T, Remme EW, Vartdal T, Pettersen E, Lunde K, Edvardsen T, Smiseth OA. Apical Rotation by Speckle Tracking Echocardiography: A Simplified Bedside Index of Left Ventricular Twist. *J Am Soc Echocardiogr* 2008.

142 Miller S, Helber U, Brechtel K, Nagele T, Hahn U, Kramer U, Hoffmeister HM, Claussen CD. MR imaging at rest early after myocardial infarction: detection of preserved function in regions with evidence for ischemic injury and non-transmural myocardial infarction. *Eur Radiol* 2003; **13**(3):498-506.

143 Saeed M, Martin AJ, Saloner D, Do L, Wilson M. Noninvasive MR characterization of structural and functional components of reperfused infarct. *Acta Radiol* 2010; **51**(10):1093-1102.

144 Taylor AJ, Al-Saadi N, bdel-Aty H, Schulz-Menger J, Messroghli DR, Friedrich MG. Detection of acutely impaired microvascular reperfusion after infarct angioplasty with magnetic resonance imaging. *Circulation* 2004; **109**(17):2080-2085.

145 Nielsen G, Fritz-Hansen T, Dirks CG, Jensen GB, Larsson HB. Evaluation of heart perfusion in patients with acute myocardial infarction using dynamic contrast-enhanced magnetic resonance imaging. *J Magn Reson Imaging* 2004; **20**(3):403-410.

146 Jerosch-Herold M, Hu X, Murthy NS, Seethamraju RT. Time delay for arrival of MR contrast agent in collateral-dependent myocardium. *IEEE Trans Med Imaging* 2004; **23**(7):881-890.

147 Skulstad H, Edvardsen T, Urheim S, Rabben SI, Stugaard M, Lyseggen E, Ihlen H, Smiseth OA. Postsystolic shortening in ischemic myocardium: active contraction or passive recoil? *Circulation* 2002; **106**(6):718-724.

148 Gjesdal O, Vartdal T, Hopp E, Lunde K, Brunvand H, Smith HJ, Edvardsen T. Left ventricle longitudinal deformation assessment by mitral annulus displacement or global longitudinal strain in chronic ischemic heart disease: are they interchangeable? *J Am Soc Echocardiogr* 2009; **22**(7):823-830.

149 Lunde K, Solheim S, Forfang K, Arnesen H, Brinch L, Bjørnerheim R, Ragnarsson A, Egeland T, Endresen K, Ilebekk A, Mangschau A, Aakhus S. Anterior myocardial infarction with acute percutaneous coronary intervention and intracoronary injection of autologous mononuclear bone marrow cells: safety, clinical outcome, and serial changes in left ventricular function during 12-months' follow-up. *J Am Coll Cardiol* 2008; **51**(6):674-676.

150 Shapiro DE. The interpretation of diagnostic tests. *Stat Methods Med Res* 1999; **8**(2):113-134.

151 Lesaffre E. Superiority, equivalence, and non-inferiority trials. *Bull NYU Hosp Jt Dis* 2008; **66**(2):150-154.

152 Thiele H, Kappl MJ, Conradi S, Niebauer J, Hambrecht R, Schuler G. Reproducibility of chronic and acute infarct size measurement by delayed enhancement-magnetic resonance imaging. *J Am Coll Cardiol* 2006; **47**(8):1641-1645.

153 Bondarenko O, Beek AM, Hofman MB, Kuhl HP, Twisk JW, van Dockum WG, Visser CA, van Rossum AC. Standardizing the definition of hyperenhancement in the quantitative assessment of infarct size and myocardial viability using delayed contrast-enhanced CMR. *J Cardiovasc Magn Reson* 2005; **7**(2):481-485.

154 Themudo RE, Johansson L, Ebeling-Barbier C, Lind L, Ahlstrom H, Bjerner T. Signal intensity of myocardial scars at delayed-enhanced MRI. *Acta Radiol* 2009; **50**(6):652-657.

155 Zhang Y, Chan AK, Yu CM, Yip GW, Fung JW, Lam WW, So NM, Wang M, Wu EB, Wong JT, Sanderson JE. Strain rate imaging differentiates transmural from non-transmural myocardial infarction: a validation study using delayed-enhancement magnetic resonance imaging. *J Am Coll Cardiol* 2005; **46**(5):864-871.

156 Barclay JL, Egred M, Kruszewski K, Nandakumar R, Norton MY, Stirrat C, Redpath TW, Walton S, Hillis GS. The relationship between transmural extent of infarction on contrast enhanced magnetic resonance imaging and recovery of contractile function in patients with first myocardial infarction treated with thrombolysis. *Cardiology* 2007; **108**(4):217-222.

157 Childs H, Ma L, Ma M, Clarke J, Cocker M, Green J, Strohm O, Friedrich MG. Comparison of long and short axis quantification of left ventricular volume parameters by cardiovascular magnetic resonance, with ex-vivo validation. *J Cardiovasc Magn Reson* 2011; **13**:40.

158 Lunde K, Solheim S, Aakhus S, Arnesen H, Abdelnoor M, Egeland T, Endresen K, Ilebekk A, Mangschau A, Fjeld JG, Smith HJ, Taraldsrud E, Grøgaard HK, Bjørnerheim R, Brekke M, Muller C, Hopp E, Ragnarsson A, Brinchmann JE, Forfang K. Intracoronary injection of mononuclear bone marrow cells in acute myocardial infarction; Supplementary appendix. 2006. http://www.nejm.org/action/showSupplements?doi=10.1056%2FNEJMoa055706&viewType=Popup&viewClass=Suppl

159 Urheim S, Edvardsen T, Torp H, Angelsen B, Smiseth OA. Myocardial strain by Doppler echocardiography. Validation of a new method to quantify regional myocardial function. *Circulation* 2000; **102**(10):1158-1164.

160 Ferferieva V, Van den BA, Claus P, Jasaityte R, Veulemans P, Pellens M, La GA, Rademakers F, Herijgers P, D'hooge J. The relative value of strain and strain rate for defining intrinsic myocardial function. *Am J Physiol Heart Circ Physiol* 2012; **302**(1):H188-H195.

161 Rademakers F, Van de WF, Mortelmans L, Marchal G, Bogaert J. Evolution of regional performance after an acute anterior myocardial infarction in humans using magnetic resonance tagging. *J Physiol* 2003; **546**(Pt 3):777-787.

162 Ryf S, Rutz AK, Boesiger P, Schwitter J. Is post-systolic shortening a reliable indicator of myocardial viability? An MR tagging and late-enhancement study. *J Cardiovasc Magn Reson* 2006; **8**(3):445-451.

163 Thorstensen A, Dalen H, Amundsen BH, Aase SA, Støylen A. Reproducibility in echocardiographic assessment of the left ventricular global and regional function, the HUNT study. *Eur J Echocardiogr* 2010; **11**(2):149-156.

164 Anwar A, Nosir Y, Alasnag M, Llemit MA, Elhagoly AA, Chamsi-Pasha H. Quantification of left ventricular longitudinal strain by two-dimensional speckle tracking: a comparison between expert and non-expert readers. *Int J Cardiovasc Imaging* 2013.

165 Amundsen BH, Crosby J, Steen PA, Torp H, Slørdahl SA, Støylen A. Regional myocardial long-axis strain and strain rate measured by different tissue Doppler and speckle tracking echocardiography methods: a comparison with tagged magnetic resonance imaging. *Eur J Echocardiogr* 2009; **10**(2):229-237.

166 de Marchi, S. F., Hopp, E., Urheim, S., Hervold, A., Murbrach, K., Massey, R., Remme, E. W., Hol, P. K., and Aakhus, S. Area strain for the assessment of myocardial infarction scar size by ultrasound 3d speckle tracking: validation with late gadolinium enhancement magnetic resonance imaging. Euroecho & other imaging modalities 2012; EUD ID: 85763.

167 Gjesdal O, Helle-Valle T, Hopp E, Lunde K, Vartdal T, Aakhus S, Smith HJ, Ihlen H, Edvardsen T. Noninvasive separation of large, medium, and small myocardial infarcts in survivors of reperfused ST-elevation myocardial infarction: a comprehensive tissue Doppler and speckle-tracking echocardiography study. *Circ Cardiovasc Imaging* 2008; **1**(3):189-96, 2.

168 Munk K, Andersen NH, Nielsen SS, Bibby BM, Bøtker HE, Nielsen TT, Poulsen SH. Global longitudinal strain by speckle tracking for infarct size estimation. *Eur J Echocardiogr* 2011; **12**(2):156-165.

169 Lipiec P, Szymczyk E, Michalski B, Stefanczyk L, Wozniakowski B, Rotkiewicz A, Szymczyk K, Kasprzak JD. Echocardiographic quantitative analysis of resting myocardial function for the assessment of viability after myocardial infarction--comparison with magnetic resonance imaging. *Kardiol Pol* 2011; **69**(9):915-922.

170 Grabka M, Wita K, Tabor Z, Paraniak-Gieszczyk B, Chmurawa J, Elzbieciak M, Bochenek T, Doruchowska-Raczek A, Trusz-Gluza M. Prediction of infarct size by speckle tracking echocardiography in patients with anterior myocardial infarction. *Coron Artery Dis* 2013; **24**(2):127-134.

171 Løgstrup BB, Høfsten DE, Christophersen TB, Møller JE, Bøtker HE, Pellikka PA, Egstrup K. Correlation between Left Ventricular Global and Regional Longitudinal Systolic Strain and Impaired Microcirculation in Patients with Acute Myocardial Infarction. *Echocardiography* 2012.

172 Crystal GJ, Downey HF, Bashour FA. Small vessel and total coronary blood volume during intracoronary adenosine. *Am J Physiol* 1981; **241**(2):H194-H201.

173 Christian TF, Rettmann DW, Aletras AH, Liao SL, Taylor JL, Balaban RS, Arai AE. Absolute myocardial perfusion in canines measured by using dual-bolus first-pass MR imaging. *Radiology* 2004; **232**(3):677-684.

174 Jerosch-Herold M, Swingen C, Seethamraju RT. Myocardial blood flow quantification with MRI by model-independent deconvolution. *Med Phys* 2002; **29**(5):886-897.

175 Morton G, Chiribiri A, Ishida M, Hussain ST, Schuster A, Indermuehle A, Perera D, Knuuti J, Baker S, Hedstrom E, Schleyer P, O'Doherty M, Barrington S, Nagel E. Quantification of absolute myocardial perfusion in patients with coronary artery disease: comparison between cardiovascular magnetic resonance and positron emission tomography. *J Am Coll Cardiol* 2012; **60**(16):1546-1555.

176 Pack NA, DiBella EV, Rust TC, Kadrmas DJ, McGann CJ, Butterfield R, Christian PE, Hoffman JM. Estimating myocardial perfusion from dynamic contrast-enhanced CMR with a model-independent deconvolution method. *J Cardiovasc Magn Reson* 2008; **10**:52.

177 Morton G, Jogiya R, Plein S, Schuster A, Chiribiri A, Nagel E. Quantitative cardiovascular magnetic resonance perfusion imaging: inter-study reproducibility. *Eur Heart J Cardiovasc Imaging* 2012.

178 Vallee JP, Lazeyras F, Kasuboski L, Chatelain P, Howarth N, Righetti A, Didier D. Quantification of myocardial perfusion with FAST sequence and Gd bolus in patients with normal cardiac function. *J Magn Reson Imaging* 1999; **9**(2):197-203.

179 Utz W, Niendorf T, Wassmuth R, Messroghli D, Dietz R, Schulz-Menger J. Contrast-dose relation in first-pass myocardial MR perfusion imaging. *J Magn Reson Imaging* 2007; **25**(6):1131-1135.

180 Lee DC, Johnson NP. Quantification of absolute myocardial blood flow by magnetic resonance perfusion imaging. *JACC Cardiovasc Imaging* 2009; **2**(6):761-770.

181 Pack NA, DiBella EV. Comparison of myocardial perfusion estimates from dynamic contrast-enhanced magnetic resonance imaging with four quantitative analysis methods. *Magn Reson Med* 2010; **64**(1):125-137.

182 Leach MO, Brindle KM, Evelhoch JL, Griffiths JR, Horsman MR, Jackson A, Jayson GC, Judson IR, Knopp MV, Maxwell RJ, McIntyre D, Padhani AR, Price P, Rathbone R, Rustin GJ, Tofts PS, Tozer GM, Vennart W, Waterton JC, Williams SR, Workman P. The assessment of antiangiogenic and antivascular therapies in early-stage clinical trials using magnetic resonance imaging: issues and recommendations. *Br J Cancer* 2005; **92**(9):1599-1610.

183 Hsu LY, Kellman P, Arai AE. Nonlinear myocardial signal intensity correction improves quantification of contrast-enhanced first-pass MR perfusion in humans. *J Magn Reson Imaging* 2008; **27**(4):793-801.

184 Bogaert J, Bosmans H, Maes A, Suetens P, Marchal G, Rademakers FE. Remote myocardial dysfunction after acute anterior myocardial infarction: impact of left ventricular shape on regional function: a magnetic resonance myocardial tagging study. *J Am Coll Cardiol* 2000; **35**(6):1525-1534.

185 Chan W, Duffy SJ, White DA, Gao XM, Du XJ, Ellims AH, Dart AM, Taylor AJ. Acute left ventricular remodeling following myocardial infarction: coupling of regional healing with remote extracellular matrix expansion. *JACC Cardiovasc Imaging* 2012; **5**(9):884-893.

186 Flacke SJ, Fischer SE, Lorenz CH. Measurement of the gadopentetate dimeglumine partition coefficient in human myocardium in vivo: normal distribution and elevation in acute and chronic infarction. *Radiology* 2001; **218**(3):703-710.

187 Larghat AM, Maredia N, Biglands J, Greenwood JP, Ball SG, Jerosch-Herold M, Radjenovic A, Plein S. Reproducibility of first-pass cardiovascular magnetic resonance myocardial perfusion. *J Magn Reson Imaging* 2013; **37**(4):865-874.

188 Elkington AG, Gatehouse PD, Ablitt NA, Yang GZ, Firmin DN, Pennell DJ. Interstudy reproducibility of quantitative perfusion cardiovascular magnetic resonance. *J Cardiovasc Magn Reson* 2005; **7**(5):815-822.

189 Jerosch-Herold M, Vazquez G, Wang L, Jacobs DR, Jr., Folsom AR. Variability of myocardial blood flow measurements by magnetic resonance imaging in the multi-ethnic study of atherosclerosis. *Invest Radiol* 2008; **43**(3):155-161.

190 Bratis K, Nagel E. Variability in quantitative cardiac magnetic resonance perfusion analysis. *J Thorac Dis* 2013; **5**(3):357-359.

191 Desch S, Eitel I, de WS, Fuernau G, Lurz P, Gutberlet M, Schuler G, Thiele H. Cardiac magnetic resonance imaging parameters as surrogate endpoints in clinical trials of acute myocardial infarction. *Trials* 2011; **12**:204.

192 Ciani O, Buyse M, Garside R, Pavey T, Stein K, Sterne JA, Taylor RS. Comparison of treatment effect sizes associated with surrogate and final patient relevant outcomes in randomised controlled trials: meta-epidemiological study. *BMJ* 2013; **346**:f457.

193 O'Regan DP, Ariff B, Baksi AJ, Gordon F, Durighel G, Cook SA. Salvage assessment with cardiac MRI following acute myocardial infarction underestimates potential for recovery of systolic strain. *Eur Radiol* 2013; **23**(5):1210-1217.

194 Kidambi A, Mather AN, Swoboda P, Motwani M, Fairbairn TA, Greenwood JP, Plein S. Relationship between Myocardial Edema and Regional Myocardial Function after Reperfused Acute Myocardial Infarction: An MR Imaging Study. *Radiology* 2013; **267**(3):701-708.

195 Korosoglou G, Humpert PM, Ahrens J, Oikonomou D, Osman NF, Gitsioudis G, Buss SJ, Steen H, Schnackenburg B, Bierhaus A, Nawroth PP, Katus HA. Left ventricular diastolic function in type 2 diabetes mellitus is associated with myocardial triglyceride content but not with impaired myocardial perfusion reserve. *J Magn Reson Imaging* 2012; **35**(4):804-811.

I

Hopp et al. Journal of Cardiovascular Magnetic Resonance 2011, 13:22
http://www.jcmr-online.com/content/13/1/22

Journal of Cardiovascular Magnetic Resonance

RESEARCH Open Access

Regional myocardial function after intracoronary bone marrow cell injection in reperfused anterior wall infarction - a cardiovascular magnetic resonance tagging study

Einar Hopp[1*], Ketil Lunde[2], Svein Solheim[3], Svend Aakhus[2], Harald Arnesen[3,4], Kolbjørn Forfang[2], Thor Edvardsen[2], Hans-Jørgen Smith[1]

Abstract

Background: Trials have brought diverse results of bone marrow stem cell treatment in necrotic myocardium. This substudy from the Autologous Stem Cell Transplantation in Acute Myocardial Infarction trial (ASTAMI) explored global and regional myocardial function after intracoronary injection of autologous mononuclear bone marrow cells (mBMC) in acute anterior wall myocardial infarction treated with percutaneous coronary intervention.

Methods: Cardiovascular magnetic resonance (CMR) tagging was performed 2-3 weeks and 6 months after revascularization in 15 patients treated with intracoronary stem cell injection (mBMC group) and in 13 controls without sham injection. Global and regional left ventricular (LV) strain and LV twist were correlated to cine CMR and late gadolinium enhancement (LGE).

Results: In the control group myocardial function as measured by strain improved for the global LV (6 months: -13.1 ± 2.4 versus 2-3 weeks: -11.9 ± 3.4%, p = 0.014) and for the infarct zone (-11.8 ± 3.0 versus -9.3 ± 4.1%, p = 0.001), and significantly more than in the mBMC group (inter-group p = 0.027 for global strain, respectively p = 0.009 for infarct zone strain). LV infarct mass decreased (35.7 ± 20.4 versus 45.7 ± 29.5 g, p = 0.024), also significantly more pronounced than the mBMC group (inter-group p = 0.034). LV twist was initially low and remained unchanged irrespective of therapy.

Conclusions: LGE and strain findings quite similarly demonstrate subtle differences between the mBMC and control groups. Intracoronary injection of autologous mBMC did not strengthen regional or global myocardial function in this substudy.

Trial registration: ClinicalTrials.gov: NCT00199823

Background

Different studies have brought diverse results on the effects of cell therapy in acute myocardial infarction. Effect measures have included clinical parameters and measurements of global left ventricular (LV) function obtained through a spectrum of methods [1-6]. Some groups have explored regional left ventricular function as evaluated by wall motion or wall thickening assessed from cardiovascular magnetic resonance (CMR) or myocardial remodeling assessed from strain echocardiography [4,7-10]. Treatment for large myocardial infarctions is considered more challenging due to risk for LV dilatation and progressive ejection fraction (EF) reduction, and in three of the studies subgroup analyses have indicated a more substantial beneficial effect from stem cell therapy in large infarctions or in hearts with low LV EF [8,9,11]. Myocardial strain calculated from CMR tagging is currently regarded as the non-invasive gold standard for assessment of regional function. However, limited availability and analysis effort seem to reduce the overall

* Correspondence: einar.hopp@oslo-universitetssykehus.no
[1]Department of Radiology, Oslo University Hospital, Rikshospitalet, Postbox 4950, Nydalen, 0424 Oslo, Norway
Full list of author information is available at the end of the article

use of the method [12,13]. In this substudy of the Autologous Stem Cell Transplantation in Acute Myocardial Infarction trial (ASTAMI) [2], we calculated LV circumferential strain and twist from short axis grid CMR tagging obtained on 28 patients first at 2-3 weeks and then subsequently 6 months after the infarction. We examined whether intracoronary injection of autologous mononuclear bone marrow cells (mBMC) influenced regional myocardial function or LV twist. In addition, we aimed to explore the potentials for tagging analysis to detect more subtle changes in myocardial function undetectable by other examination techniques in routine use.

Methods

Study group

Methods and techniques used in the ASTAMI trial have been reported in detail previously [2]. Briefly, 100 patients with acute left anterior descending artery (LAD) myocardial infarction were randomized to either intracoronary injection of autologous mBMC (mBMC group) or control with no sham injection after successful revascularization. mBMC injection was performed 4-8 days (mean 6 days) after percutaneous coronary intervention (PCI). Baseline CMR was performed after 2-3 weeks (18.8 ± 3.8 days) after myocardial infarction and was repeated after 6 months. For this substudy, the CMR protocol included short axis grid tagging sequences in addition to cine images and post contrast late gadolinium enhancement (LGE). The patients were a consecutive series of the last 28 patients included in ASTAMI who either received mBMC per protocol (n = 15) or belonged to the control group (n = 13). The study complies with the Declaration of Helsinki, and the protocol was approved by the regional committee for research ethics. All patients gave written, informed consent.

Cardiac Magnetic Resonance

Cine images, tagging sequences and late enhancement images were acquired in the same image session with 1.5 tesla units (Magnetom Vision Plus or Magnetom Sonata, Siemens, Erlangen, Germany) with a phased array body coil.

Two cine long axis projections of the left ventricle were acquired with either a breath-hold segmented spoiled gradient echo sequence, fast low angle shot (FLASH) or a breath-hold segmented balanced gradient echo sequence, fast imaging with steady-state free precession (trueFISP). Each patient had either paired FLASH or paired trueFISP examinations. Temporal resolution was 50 ms or less and slice thickness was 6 mm.

Tagged CMR of the left ventricle was obtained with a FLASH sequence. Three short axis levels were standardized with the basal level just apical to the mitral ring at end-systole, the mid-ventricular level on the mid-point of the left ventricular long axis, and apical level just basal to the level of luminal closure at end-systole. Orthogonal tags in a grid pattern were parallel or perpendicular to the 2-chamber long axis plane with distance between tags of 8 mm. Temporal resolution was less than 50 ms and slice thickness 6 or 8 mm.

Late enhancement images were obtained 10 - 20 minutes after intravenous injection of 0.2 mmol/kg gadopentetate dimeglumine (Magnevist, Schering, Berlin, Germany) in two long axis projections corresponding to the cine images and multiple short axis projections covering the LV with a breath-hold inversion recovery turbo gradient echo sequence. The inversion time was chosen to null the signal of the normal myocardium. Slice thickness was 7 or 8 mm and increment between slices was 10 mm.

CMR analysis

All CMR analyses were performed blinded to treatment allocation. End diastolic volumes (EDV), end systolic volumes (ESV) and EF were calculated according to the biplane area-length method from the two long axis cine projections [14].

Tagging recordings were analyzed with Harmonic Phase Imaging (HARP version 1.0, Diagnosoft Inc, Palo Alto, California). For each slice, 24 mid-wall points were semi-automatically tracked, and circumferential Lagrangian end systolic strain was calculated from deformation of the line between points. Each of the 24 strain measurements were manually assigned to the 16 segment model [15], and mean strain was obtained for all segments, selected LV regions and the global LV. By convention negative strain indicates myocardial shortening. Typical segmental tagging analysis of an apical slice is illustrated in Figure 1.

Segments were excluded for further analysis if more than half of the segment's strain curves had been excluded due to noise. The LV regions were excluded for further analysis if more than half of the segments in the region had been excluded. Global mean strain values were excluded if more than 50% of the segments had been excluded or if either the basal, mid-ventricular or apical slices suffered from missing segmental data.

LV rotation data were obtained from the mid-wall tracking also made for strain analysis in the basal and apical slices, values given in degrees. LV twist was calculated as basal rotation subtracted from apical rotation. Strain and twist inter- and intra-observer reproducibility was assessed through repeated analyses of 10 randomly chosen tagging examinations.

Late enhancement short axis slices were manually assigned to basal, mid or apical left ventricular slices and divided into sectors to fit the 16 segment model [15]. Myocardial borders and the enhancing areas were

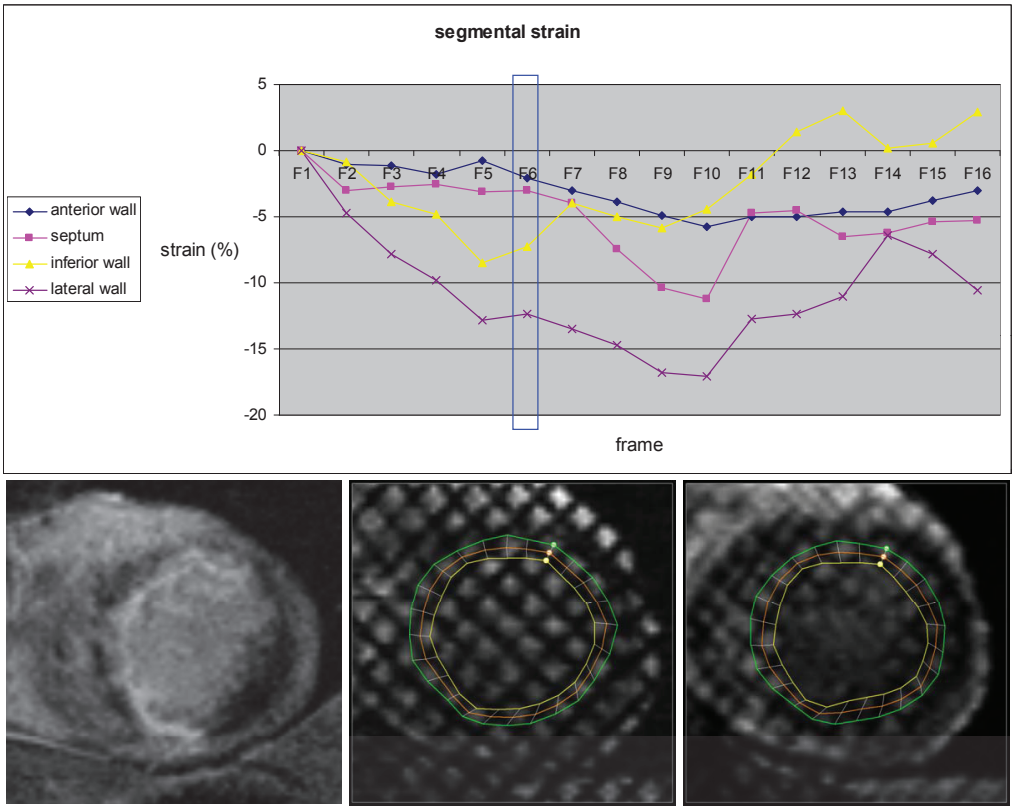

Figure 1 Baseline apical tagging analysis in a 49 year old male patient in the mBMC group. Upper part: The curves represent strain in the apical segments, analyzed with HARP software from a short axis CMR tagging sequence. The vertical box represents the end systolic frame (F6). There is almost normal function in the lateral wall, dysfunction in the inferior wall, while septum and the anterior wall are almost akinetic with possible post-systolic contraction. Note increasing noise during diastolic frames, due to T1 relaxation of the tagged myocardium. Lower part: Left: Short axis apical LGE image with hyperintensity in the anterior wall, septum and part of the inferior wall. Mid and right: Short axis apical end diastolic (mid) and end systolic (right) tagging images with application of the semi-automatically traced lines from HARP software. Circumferential mid-wall end systolic strain was calculated from deformation of the orange mid-wall line.

manually delineated (PACS, Sectra, Sweden) [12,16-18]. Absolute and relative myocardial infarct volumes were obtained for each segment. Myocardial and infarct masses were converted from volume by multiplying by 1.05 g/ml [19].

LGE and strain data were analyzed globally and in corresponding LV regions, based on baseline LGE findings. All infarct segments in each patient were summarized, denoted infarct zone. All segments without late enhancement were denoted remote segments. Segments with more than 75% infarct were studied selectively, denoted transmural infarct zone, corresponding to the transmurally infarcted segments studied by Herbots et al. [8].

Statistics

Categorical variables were analyzed with the chi-square test. Continuous data are presented as mean ± standard deviation, and in the gross material all variables for baseline and end-point analyses approximated a normal distribution. For comparisons between groups at baseline two-sample t-tests were performed. Intra-group changes were evaluated by paired sample t-tests. Development between 2-3 weeks and 6 months was assessed by analysis of covariance, with the baseline values used as a covariate. Corresponding analyses were performed on patients with lower than median EF at baseline CMR. Owing to the relatively low number of patients inter-group comparisons were performed with the

non-parametric Mann-Whitney test and intra-group change was evaluated with the Wilcoxon signed ranks test. For tagging reproducibility two-way mixed absolute agreement intraclass correlation analyses of global and regional strain and twist were performed. The intraclass correlation coefficients (ICC) are presented with 95% confidence interval. SPSS software version 16.0 was used. Tests were two-sided, and p-values < 0.05 were considered statistically significant.

Results

Patient characteristics and LV measurements

Among all patients, the mean age was 58.6 ± 9.1 years, mean time from the onset of symptoms to PCI was 234 ± 104 minutes, and the mean value for maximum creatine kinase MB was 361 ± 136 μg per liter. The characteristics of the patients at admission did not differ significantly between the two groups (Table 1).

The results of volumetric, LGE, strain and twist analyses for all patients are summarized in Table 2, and selected results for the group of patients with baseline EF lower than median (51.9%) are summarized in Table 3. At baseline, there were no significant differences between the groups for EF, ESV, EDV, LV mass, infarct size, LV strain or LV twist, and there were no significant differences in myocardial mass, infarct mass, infarct percent or strain in the LV regions examined.

EDV and ESV did not change over time, but there was a trend towards increased EF from the baseline examination to 6 months, irrespective of treatment allocation. In the subgroup of patients with low baseline EF, EF increased significantly (43.7 ± 7.2 to 51.9 ± 8.8%, p = 0.042) and ESV decreased significantly (114.8 ± 38.1 to 95.2 ± 43.6 ml, p = 0.043) in the control group but did not change in the mBMC group.

Late gadolinium enhancement

Average segmental LGE at baseline is illustrated in Figure 2a. All 448 segments in all 28 patients were included for LGE analysis at both time points. The individual LV infarct percent at baseline ranged from 2.2% to 50.1%. Ten patients had small (< 18%), 9 had intermediate (18-30%) and 9 had large infarcts (> 30%) [20]. A total of 271 segments were judged as partially or completely infarcted at baseline, respectively 266 at 6 months. The infarcts affected the basal segments of LV in 15 patients only; 14 of these had large and medium-sized infarcts. In all but 1 patient the infarct involved at least 1 segment outside the presumed LAD supplying territory [15]. In the mid-ventricular part of LV, there was LGE in the inferior septum in 26 patients and in the anterior lateral wall in 23 patients. In the apical part the inferior and lateral segments were infarcted in 27 and 24 patients, respectively. LV infarct mass and infarct percent decreased significantly from baseline to 6 months in the control group only, and there was significant difference between the mBMC and control groups. Regionally, infarct percent decreased significantly in the infarct zone of the control group, and in the transmural infarct zone of both groups. Infarct mass of the infarct zone decreased significantly more in the control group than in the mBMC group. In the group of patients with low baseline EF, infarct percent in the infarct zone decreased more in the controls than in the mBMC patients.

LV function

Average segmental strain at baseline is illustrated in Figure 2b. Forty-six segments were excluded for strain analysis at baseline, and 35 segments were excluded at 6 months. LV strain was analyzed in 26 patients. Regionally, infarct zone strain and strain of remote

Table 1 Patient characteristics at admission

	mBMC (n = 15)	Controls (n = 13)	p-value
Age - years	58.5 ± 8.9	58.7 ± 9.7	0.965
Female sex - no	3	3	0.843
Body mass index	25.7 ± 2.6	27.1 ± 3.2	0.240
Current smokers - no	5	3	0.836
Hypertension - no	2	3	0.502
Diabetes mellitus - no	1	1	0.916
Previous angina - no	2	4	0.262
Blood pressure - mm Hg			
systolic	133 ± 21	125 ± 18	0.320
diastolic	79 ± 12	78 ± 13	0.807
Heart rate - beats/min	71 ± 12	80 ± 14	0.090
Time from symptom onset to PCI - min	239 ± 100	228 ± 112	0.780
Maximum creatine kinase MB - μg/l	382 ± 130	334 ± 143	0.376

Table 2 Global and regional results; all patients (n = 28)

		Baseline			6 months		
		mBMC	controls	p-value 1	mBMC	controls	p-value 2
Left ventricle N = 28	EDV - ml	175.1 ± 48.7	176.8 ± 52.8	0.932	174.9 ± 60.0	174.3 ± 62.3	0.828
	ESV - ml	91.2 ± 35.2	84.9 ± 41.0	0.668	87.6 ± 44.9	78.0 ± 42.3	0.674
	EF - %	49.3 ± 9.5	54.1 ± 11.3	0.233	52.4 ± 11.9	57.9 ± 10.1	0.610
	LV mass - g	168.6 ± 28.3	171.5 ± 42.1	0.831	162.4 ± 30.8	160.4 ± 41.1*	0.379
	infarct mass - g	38.6 ± 23.3	45.7 ± 29.5	0.484	37.6 ± 20.5	35.7 ± 20.4*	0.034
	infarct percent - %	22.1 ± 12.4	26.4 ± 14.8	0.410	22.2 ± 10.8	22.0 ± 11.0*	0.026
	global strain - %	-11.1 ± 2.4	-11.9 ± 3.4	0.512	-11.1 ± 2.6	-13.1 ± 2.4*	0.027
	twist - °	11.3 ± 3.6	12.8 ± 5.4	0.365	12.6 ± 4.3	11.8 ± 3.7	0.411
Infarct zone N = 27	mass - g	103.0 ± 39.6	103.9 ± 37.6	0.955	100.3 ± 39.9	96.2 ± 34.5*	0.217
	infarct mass - g	38.6 ± 23.3	45.7 ± 29.5	0.484	37.6 ± 20.5	35.7 ± 20.4*	0.034
	infarct percent - %	34.4 ± 13.6	41.5 ± 17.7	0.242	34.3 ± 12.6	35.0 ± 11.6*	0.084
	strain - %	-9.7 ± 3.4	-9.3 ± 4.1	0.770	-10.2 ± 3.3	-11.8 ± 3.0*	0.009
Transmural infarct zone N = 13	mass - g	32.3 ± 22.6	35.0 ± 26.2	0.855	33.7 ± 21.4	33.6 ± 24.0	0.519
	infarct mass - g	29.0 ± 23.0	32.5 ± 25.2	0.804	26.6 ± 17.7	26.1 ± 19.5	0.468
	infarct percent - %	86.8 ± 7.4	90.3 ± 6.1	0.377	77.6 ± 4.3*	76.6 ± 11.4*	0.401
	strain - %	-2.0 ± 1.5	-6.6 ± 5.6	0.107	-2.4 ± 1.4	-8.6 ± 4.9	0.108
Remote segments N = 27	mass - g	64.4 ± 22.1	66.5 ± 24.3	0.816	61.1 ± 22.8	63.2 ± 24.0	0.965
	strain - %	-14.4 ± 2.4	-14.9 ± 2.3	0.560	-14.3 ± 3.3	-15.6 ± 2.3	0.195

p-value 1 refers to between group differences at baseline (two sample t-test). p-value 2 refers to between group differences in changes from baseline (analysis of covariance). *p < 0.05 for intra-group changes from baseline, evaluated by paired sample t-test.

segments were analyzed in 27 patients. Thirteen patients had 1 or more segments with more than 75% infarct, and all were included for transmural infarct zone strain analyses. The ICC of agreement for inter-observer judgments was 0.97 (0.87-0.99) for global strain, 0.96 (0.83-0.99) for infarct zone strain and 0.95 (0.65-0.99) for transmural infarct zone strain. Corresponding ICC of agreement for intra-observer observations was 0.99 (0.95-1.00), 0.98 (0.81-0.99) and 0.96 (0.82-0.99) respectively. For individual segments agreement was lower with an ICC of 0.81 (0.75-0.86) for intra-observer and 0.87 (0.83-0.91) for inter-observer judgments.

LV function as measured by global strain improved significantly from baseline to 6 months in the control group (from -11.9 ± 3.4 to -13.1 ± 2.4%, p = 0.014), but remained unchanged in the mBMC group. In the control group, regional myocardial function improved significantly in the infarct zone (from -9.3 ± 4.1 to -11.8 ± 3.0%, p = 0.001),

Table 3 Selected results; patients with baseline EF < median (51.9%)

		Baseline			6 months		
		mBMC	controls	p-value 1	mBMC	controls	p-value 2
Left ventricle N = 14	EDV - ml	183.2 ± 46.1	202.9 ± 49.3	0.641	194.6 ± 64.4	191.6 ± 55.6	0.162
	ESV - ml	105.1 ± 33.1	114.8 ± 38.1	0.640	107.7 ± 43.4	95.2 ± 43.6*	0.028
	EF - %	43.3 ± 6.4	43.7 ± 7.2	0.947	45.8 ± 7.1	51.9 ± 8.8*	0.386
	infarct percent - %	28.8 ± 10.7	33.5 ± 12.1	0.505	27.2 ± 8.8	28.7 ± 12.1*	0.071
	global strain - %	-10.0 ± 2.4	-11.3 ± 2.9	0.536	-11.4 ± 2.8	-13.0 ± 2.8	0.189
Infarct zone N = 14	infarct percent - %	41.0 ± 12.4	46.6 ± 11.9	0.463	37.9 ± 10.1*	38.8 ± 11.4*	0.053
	strain - %	-8.7 ± 2.9	-8.9 ± 2.7	0.738	-9.9 ± 3.1	-11.7 ± 2.4*	0.205
Transmural infarct zone N = 9	infarct percent - %	86.8 ± 7.4	90.5 ± 7.7	0.462	77.6 ± 4.3*	79.2 ± 12.7	0.327
	strain - %	-2.0 ± 1.5	-4.6 ± 4.9	0.221	-2.4 ± 1.4	-8.6 ± 5.9	0.027

p-value 1 refers to between group differences at baseline (Mann-Whitney). p-value 2 refers to between group differences in changes from baseline (Mann-Whitney). *p < 0.05 for intra-group differences from baseline, evaluated by Wilcoxon signed rank test.

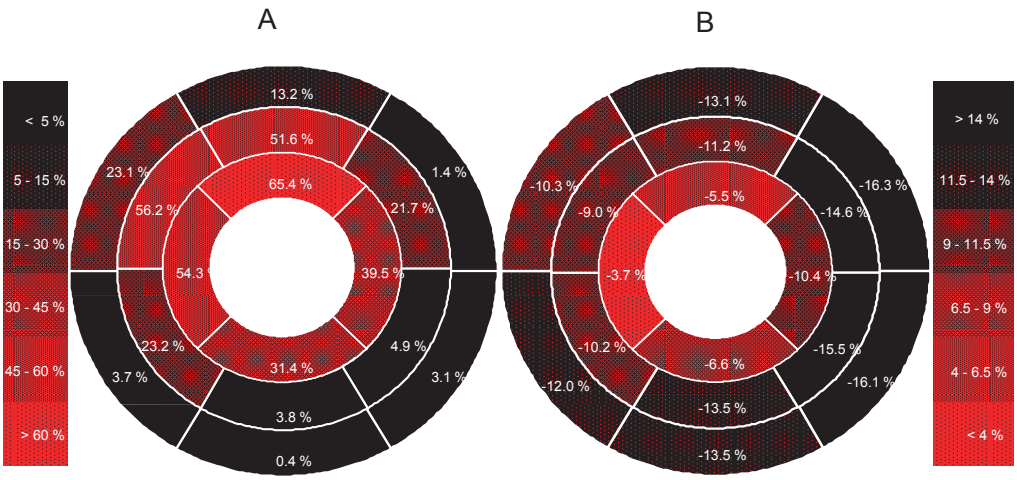

Figure 2 Bull's eye plots over baseline LGE and strain in the 16 LV segments model. 2 a: Average infarct involvement (percent) in each segment (n = 448). 2 b: Average strain (percent) in each segment (n = 402). Negative strain values indicate myocardial shortening, and a strain value with amplitude higher than -14% is considered normal.

but not in the transmural infarct zone or the remote segments. Regional myocardial function remained unchanged in the mBMC patients. In the group of patients with low baseline EF, strain improvement was significantly more pronounced for the controls in the transmural infarct zone only. LV twist was analyzed in all 28 patients. Twist was low at baseline for both groups, and did not change significantly over time in either of the groups. The ICC of agreement for inter-observer judgments was 0.92 (0.74-0.98) and for intra-observer observations 0.96 (0.85-0.99).

The changes of LV strain in the control group correlated significantly with LV infarction mass at baseline and change of LV infarction mass (Table 4).

Discussion

The ASTAMI study, which included 100 patients, was originally designed with a power of 80% to reveal a potential difference of 5% points of LV EF development between the mBMC and the control groups as measured by single-photon-emission computed tomography. No difference was found for global functional development or for clinical parameters [2,21]. For LV EF inter-observer variability was assessed with ICC of 0.85 (0.67-0.93) for FLASH cines and ICC of 0.98 (0.96-0.99) for trueFisp cines [2] (Supplementary Appendix). In this substudy, only 28 patients were included, resulting in reduced power. Unlike previous reports, myocardial wall function developed beneficially for the control group as compared with the mBMC group. Strain improvement was 2.5 ± 2.0% points in the infarct zone and 1.6 ± 1.8% points globally. Infarct mass as shown by LGE developed similarly to strain, with a more pronounced infarct mass reduction for the controls than for the mBMC group. Both groups had a parallel, but statistically non-significant trend towards LV EF improvement. The results from this study illuminate the potentials for detailed regional myocardial examination to detect subtle differences of myocardial function not always detected by other examination techniques routinely used.

Care must be taken drawing conclusions from the results regarding development of myocardial function and LGE in this study. Recently, Beitnes et al. published results from the long-term follow-up of the ASTAMI trial including global and regional LAD strain analyses performed with longitudinal two-dimensional speckle-tracking echocardiography (2D STE) [10]. They reported a significant improvement of regional and global peak systolic strain from baseline to 6 months, which was maintained at three years post-infarction. However,

Table 4 Correlation between strain development and infarct mass in controls

	Beta (standardized)	R	p-value
LV infarct mass at baseline	-0.663	0.663	0.019
Change of infarct mass	0.665	0.665	0.018
Dependent variable: change of LV strain			

Linear regression analysis for correlation between change of LV strain (dependent) and baseline LV infarct mass and change of LV infarct mass in controls (n = 12).

there were no significant differences between the groups regarding change in myocardial systolic or diastolic function. The present substudy introduces some methodological refinement to this study. Circumferential strain was calculated from short axis CMR tagging versus longitudinal strain calculation from long axis 2D STE. For the regional CMR tagging analysis the infarct zone was directly defined by findings from baseline LGE, achieved during the same image session. Inter- and intra-observer strain reproducibility was excellent for global and regional strain analyses, even though reproducibility decreased when strain was studied on the individual segmental level. For the echo examination there was no opportunity to directly delineate the myocardial infarct area, and the region studied was the predefined LAD territory. Additionally, strain calculations were made at different time points. Baseline of the echo study was 4.5 ± 1.1 days after the myocardial infarction, before the bone marrow aspiration and intracoronary mBMC injection of the mBMC group, whereas the baseline CMR examination was performed at 18.8 ± 3.8 days. This fact is also relevant for the comparison of the global LV volumetric analyses. Even though the groups did not develop significantly differently, the CMR examinations in the main ASTAMI study revealed a larger increase of LV EF (1.2% vs 4.3%, p = 0.054), and a larger decrease of infarct size (-2.3 vs -5.9 ml, p = 0.11) in the control group than the mBMC group [2]. There were no between-group differences in baseline infarct mass in the larger, main ASTAMI study. Although not significant, the baseline infarct mass in the substudy was slightly, but not significantly higher in the control group than in the mBMC group. Strain values in the ischemic heart are closely related to LGE [22-24], and strain improves over time after acute myocardial infarction [25]. In the present study, there was a significant correlation between improvement of strain and reduction of infarct size in the control group (Table 4). Part of the differences between the study groups may have been caused by the small study group bias.

In the main ASTAMI study, 72% of the patients who received intracoronary cell injections reported mild chest pain during the procedure and 77% had transient ischemic ST deviation during balloon inflation. No patient had reinfarction related to the procedure [2]. Beitnes et al. recently reported no adverse effects observed after three years in the same population [21]. Thus, there is no indication that the intracoronary balloon inflation procedure has influenced the clinical results of the mBMC group. The present study was not designed to reveal any subtle immediate beneficial or unfavorable changes in the myocardium after intracoronary injection of mBMC. One might speculate, however, that recurrent balloon inflations might negatively influence myocardial function in the treatment perfusion area, as indicated in our results.

Regional wall function has been investigated by different means in other stem cell trials. In the Repair-AMI trial regional function improved more in infarcted areas in the stem cell group judged by the centerline chord method at 4 months [6]. In a recent CMR substudy by Dill et al., infarct area wall thickening was assessed by cine CMR examination, and the results indicated more pronounced increase of wall thickening in the stem cell group after 12 months in the group of patients with initial EF lower than median EF (48.9%) [9]. In the BOOST trial, wall thickening and wall motion in infarcted areas were studied by short axis cine CMR. There was no significant treatment effect from stem cell injection on global LVEF or on the regional function parameters studied at 18 months or 5 years follow up [7,26]. In the trial from Leuven wall thickening was assessed by short axis cine CMR in transmurally and non-transmurally infarcted segments. The change in systolic function did not differ at 4 months between the stem cell group and the placebo group [5]. However, there was a beneficial stem cell treatment effect on strain as measured by tissue Doppler imaging for segments with initial LGE involvement of more than 75% [8]. The results from our substudy do not support any potential beneficial effect from intracoronary injection of mBMC after reperfused myocardial infarction. This also applies to the patients with larger transmural myocardial infarcts and those with low EF.

End systolic LV twist is the difference in the systolic clockwise rotational movement of the basal region from the counter-clockwise rotational movement of the apical region as seen from the apex. The rotation is part of the complex wringing movement of the left ventricle during systole [27,28]. Baseline end systolic LV twist values in our study were 11.3 ± 3.6°and 12.8 ± 5.4°in the mBMC group and controls, respectively. Despite lack of healthy controls for comparison, we regard these values to be clearly lower than the normal values as measured by speckle-tracking echocardiography [29,30]. Reproducibility was excellent, with ICC of 0.92 and 0.96 for inter- and intra-observer variability, respectively. Several authors have found reduced twist in acute or chronic myocardial ischemia compared with twist in healthy individuals, and twist reduction is correlated to the extent of LV EF reduction [29,31,32]. Twist and the more simplified apical torsion have been suggested as reliable and sensitive tools to detect LV dysfunction. In a patient group of acute LAD myocardial infarction, Han et al. found a positive correlation between LV EF and twist, and in addition twist significantly improved one month after revascularization, parallel to a mean EF increase from 38.8% to 49.7% [33]. In the present study

mean baseline EF was higher. Further studies, also differentiating smaller from larger infarctions, are needed to evaluate potentials and clinical significance for twist development after acute myocardial infarction.

According to the standardized scheme for myocardial territory assignment the LAD artery supplies the anterior wall and the anterior part of the septum, as well as the apical septum and the apical cap [15]. Ortiz-Pérez et al. have suggested a modification to this scheme, adding the mid anterolateral segment and the apical lateral and inferior segments to the LAD territory [34]. Individual variation will add complexity to these schemes in any patient studies. In the present study, only patients with their first ST-elevation anterior wall infarction were included. Small, medium-sized and large infarcts were quite evenly represented. The relative lack of basal slice LGE in the small infarcts probably was a consequence of the site for LAD occlusion. In the mid-ventricular slices LGE of the anterior lateral wall and the inferior part of the septum was of similar magnitude, and quite significant. Visually, the LGE areas of these segments were fringes of the LGE in the neighboring LAD territory segments. In the apical slices all segments were largely affected, supporting the modification suggested by Ortiz-Pérez et al. [34]. As illustrated in Figure 2 average reduction of segmental strain followed a pattern similar to the average LGE involvement, although strain values were relatively lower in the septum.

Limitations

The time point for the baseline CMR at least two weeks after the acute event was chosen to reduce overestimation of infarct size owing to tissue edema, and T2-weighted sequences for evaluation of edema were therefore not part of our protocol. Obviously, more information on LV volumes and function could have been available with an additional CMR examination before or immediately after intracoronary cell injection. Thus, we may have missed early and short term changes after the injection, and thereby possible differences between the groups, either related to stem cell effect, or even to the intracoronary balloon inflation procedure itself. This fact also is relevant for the direct comparison between echo and CMR results. However, the time point for baseline CMR examination was suitable for the investigation of myocardial remodeling after the acute phase. Serial CMR studies underscore the advantages of examining LGE after the first 7 days of resorption of necrotic myocardium and hemorrhage, reduction of myocardial edema and possibly rescue of myocardium at risk. A better correlation was found between later functional parameters and LGE after one week compared with LGE immediately after the infarction and reperfusion [35-37].

Short duration of follow-up and a relatively small number of patients, even reduced by exclusions from tagging noise; make the present study insufficient in the assessment of post mBMC treatment effects. LV EF was examined with the area-length method, possibly adding variability compared with multiple short-axis cines. Differences in development may have been masked. The selection of patients did not completely concur with the main ASTAMI study, with a non-significant, numerically slightly higher initial infarct mass in the control group than the mBMC group.

Conclusions

The results from the present study do not support the hypothesis that intracoronary mBMC injection after reperfused anterior wall infarction reduces infarct size or improves myocardial function. Findings from regional LGE and strain analyses quite similarly demonstrate subtle differences between the mBMC and control groups with a slightly more favorable development in the controls. The potential role for LV twist as assessed by CMR tagging has to be evaluated in further studies.

Acknowledgements

Dr. Ketil Lunde and Dr. Svein Solheim were supported by research fellowships from the Norwegian Council on Cardiovascular Diseases.

Author details

[1]Department of Radiology, Oslo University Hospital, Rikshospitalet, Postbox 4950, Nydalen, 0424 Oslo, Norway. [2]Department of Cardiology, Oslo University Hospital, Rikshospitalet, Norway. [3]Department of Cardiology, Oslo University Hospital, Ullevål, Norway. [4]Faculty of Medicine, University of Oslo, Oslo, Norway.

Authors' contributions

EH carried out CMR examinations, image analysis and drafted the manuscript. KL and SS coordinated the study. HA, KF and SA participated in the study design. TE participated in the study design and strain analysis. HJS participated in the study design and CMR analysis. All authors have made revisions to the manuscript and have read and approved the final version.

Competing interests

The authors declare that they have no competing interests.

Received: 17 November 2010 Accepted: 17 March 2011
Published: 17 March 2011

References

1. Nogueira FB, Silva SA, Haddad AF, Peixoto CM, Carvalho RM, Tuche FA, Soares VE, Sousa AL, Rabischoffsky A, Mesquita CT, Borojevic R, Dohmann HF: **Systolic function of patients with myocardial infarction undergoing autologous bone marrow transplantation.** *Arq Bras Cardiol* 2009, **93**:374-72.
2. Lunde K, Solheim S, Aakhus S, Arnesen H, Abdelnoor M, Egeland T, Endresen K, Ilebekk A, Mangschau A, Fjeld JG, Smith HJ, Taraldsrud E, Grogaard HK, Bjornerheim R, Brekke M, Muller C, Hopp E, Ragnarsson A, Brinchmann JE, Forfang K: **Intracoronary injection of mononuclear bone marrow cells in acute myocardial infarction.** *N Engl J Med* 2006, **355**:1199-1209.
3. Wollert KC, Meyer GP, Lotz J, Ringes-Lichtenberg S, Lippolt P, Breidenbach C, Fichtner S, Korte T, Hornig B, Messinger D, Arseniev L, Hertenstein B, Ganser A, Drexler H: **Intracoronary autologous bone-**

marrow cell transfer after myocardial infarction: the BOOST randomised controlled clinical trial. *Lancet* 2004, **364**:141-148.

4. van der Laan A, Hirsch A, Nijveldt R, van d V, van der Giessen WJ, Doevendans PA, Waltenberger J, Ten Berg JM, Aengevaeren WR, Zwaginga JJ, Biemond BJ, van Rossum AC, Tijssen JG, Zijlstra F, Piek JJ: **Bone marrow cell therapy after acute myocardial infarction: the HEBE trial in perspective, first results.** *Neth Heart J* 2008, **16**:436-439.
5. Janssens S, Dubois C, Bogaert J, Theunissen K, Deroose C, Desmet W, Kalantzi M, Herbots L, Sinnaeve P, Dens J, Maertens J, Rademakers F, Dymarkowski S, Gheysens O, Van Cleemput J, Bormans G, Nuyts J, Belmans A, Mortelmans L, Boogaerts M, Van de Werf F: **Autologous bone marrow-derived stem-cell transfer in patients with ST-segment elevation myocardial infarction: double-blind, randomised controlled trial.** *Lancet* 2006, **367**:113-121.
6. Schachinger V, Erbs S, Elsasser A, Haberbosch W, Hambrecht R, Holschermann H, Yu J, Corti R, Mathey DG, Hamm CW, Suselbeck T, Assmus B, Tonn T, Dimmeler S, Zeiher AM: **Intracoronary bone marrow-derived progenitor cells in acute myocardial infarction.** *N Engl J Med* 2006, **355**:1210-1221.
7. Meyer GP, Wollert KC, Lotz J, Steffens J, Lippolt P, Fichtner S, Hecker H, Schaefer A, Arseniev L, Hertenstein B, Ganser A, Drexler H: **Intracoronary bone marrow cell transfer after myocardial infarction: eighteen months' follow-up data from the randomized, controlled BOOST (BOne marrOw transfer to enhance ST-elevation infarct regeneration) trial.** *Circulation* 2006, **113**:1287-1294.
8. Herbots L, D'hooge J, Eroglu E, Thijs D, Ganame J, Claus P, Dubois C, Theunissen K, Bogaert J, Dens J, Kalantzi M, Dymarkowski S, Bijnens B, Belmans A, Boogaerts M, Sutherland G, Van deWerf F, Rademakers F, Janssens S: **Improved regional function after autologous bone marrow-derived stem cell transfer in patients with acute myocardial infarction: a randomized, double-blind strain rate imaging study.** *Eur Heart J* 2009, **30**:662-670.
9. Dill T, Schachinger V, Rolf A, Mollmann S, Thiele H, Tillmanns H, Assmus B, Dimmeler S, Zeiher AM, Hamm C: **Intracoronary administration of bone marrow-derived progenitor cells improves left ventricular function in patients at risk for adverse remodeling after acute ST-segment elevation myocardial infarction: results of the Reinfusion of Enriched Progenitor cells And Infarct Remodeling in Acute Myocardial Infarction study (REPAIR-AMI) cardiac magnetic resonance imaging substudy.** *Am Heart J* 2009, **157**:541-547.
10. Beitnes JO, Gjesdal O, Lunde K, Solheim S, Edvardsen T, Arnesen H, Forfang K, Aakhus S: **Left ventricular systolic and diastolic function improve after acute myocardial infarction treated with acute percutaneous coronary intervention, but are not influenced by intracoronary injection of autologous mononuclear bone marrow cells: a 3 year serial echocardiographic sub-study of the randomized-controlled ASTAMI study.** *Eur J Echocardiogr* 2011, **12**:98-106.
11. Schaefer A, Zwadlo C, Fuchs M, Meyer GP, Lippolt P, Wollert KC, Drexler H: **Long-term effects of intracoronary bone marrow cell transfer on diastolic function in patients after acute myocardial infarction: 5-year results from the randomized-controlled BOOST trial–an echocardiographic study.** *Eur J Echocardiogr* 2010, **11**:165-171.
12. Edvardsen T, Rosen BD: **Why do we need magnetic resonance imaging in cardiology?** *Scand Cardiovasc J* 2005, **39**:260-263.
13. Shehata ML, Cheng S, Osman NF, Bluemke DA, Lima JA: **Myocardial tissue tagging with cardiovascular magnetic resonance.** *J Cardiovasc Magn Reson* 2009, **11**:55.
14. Sievers B, Brandts B, Franken U, Trappe HJ: **Single and biplane TrueFISP cardiovascular magnetic resonance for rapid evaluation of left ventricular volumes and ejection fraction.** *J Cardiovasc Magn Reson* 2004, **6**:593-600.
15. Cerqueira MD, Weissman NJ, Dilsizian V, Jacobs AK, Kaul S, Laskey WK, Pennell DJ, Rumberger JA, Ryan T, Verani MS: **Standardized myocardial segmentation and nomenclature for tomographic imaging of the heart: a statement for healthcare professionals from the Cardiac Imaging Committee of the Council on Clinical Cardiology of the American Heart Association.** *Circulation* 2002, **105**:539-542.
16. Kim RJ, Fieno DS, Parrish TB, Harris K, Chen EL, Simonetti O, Bundy J, Finn JP, Klocke FJ, Judd RM: **Relationship of MRI delayed contrast enhancement to irreversible injury, infarct age, and contractile function.** *Circulation* 1999, **100**:1992-2002.
17. Schuijf JD, Kaandorp TA, Lamb HJ, van der Geest RJ, Viergever EP, van der Wall EE, de RA, Bax JJ: **Quantification of myocardial infarct size and transmurality by contrast-enhanced magnetic resonance imaging in men.** *Am J Cardiol* 2004, **94**:284-288.
18. Bondarenko O, Beek AM, Hofman MB, Kuhl HP, Twisk JW, van Dockum WG, Visser CA, van Rossum AC: **Standardizing the definition of hyperenhancement in the quantitative assessment of infarct size and myocardial viability using delayed contrast-enhanced CMR.** *J Cardiovasc Magn Reson* 2005, **7**:481-485.
19. Shapiro EP, Rogers WJ, Beyar R, Soulen RL, Zerhouni EA, Lima JA, Weiss JL: **Determination of left ventricular mass by magnetic resonance imaging in hearts deformed by acute infarction.** *Circulation* 1989, **79**:706-711.
20. Wu KC, Zerhouni EA, Judd RM, Lugo-Olivieri CH, Barouch LA, Schulman SP, Blumenthal RS, Lima JA: **Prognostic significance of microvascular obstruction by magnetic resonance imaging in patients with acute myocardial infarction.** *Circulation* 1998, **97**:765-772.
21. Beitnes JO, Hopp E, Lunde K, Solheim S, Arnesen H, Brinchmann JE, Forfang K, Aakhus S: **Long-term results after intracoronary injection of autologous mononuclear bone marrow cells in acute myocardial infarction: the ASTAMI randomised, controlled study.** *Heart* 2009, **95**:1983-1989.
22. Gjesdal O, Hopp E, Vartdal T, Lunde K, Helle-Valle T, Aakhus S, Smith HJ, Ihlen H, Edvardsen T: **Global longitudinal strain measured by two-dimensional speckle tracking echocardiography is closely related to myocardial infarct size in chronic ischaemic heart disease.** *Clin Sci (Lond)* 2007, **113**:287-296.
23. Cupps BP, Bree DR, Wollmuth JR, Howells AC, Voeller RK, Rogers JG, Pasque MK: **Myocardial viability mapping by magnetic resonance-based multiparametric systolic strain analysis.** *Ann Thorac Surg* 2008, **86**:1546-1553.
24. Vartdal T, Brunvand H, Pettersen E, Smith HJ, Lyseggen E, Helle-Valle T, Skulstad H, Ihlen H, Edvardsen T: **Early prediction of infarct size by strain Doppler echocardiography after coronary reperfusion.** *J Am Coll Cardiol* 2007, **49**:1715-1721.
25. Rademakers F, Van de WF, Mortelmans L, Marchal G, Bogaert J: **Evolution of regional performance after an acute anterior myocardial infarction in humans using magnetic resonance tagging.** *J Physiol* 2003, **546**:777-787.
26. Meyer GP, Wollert KC, Lotz J, Pirr J, Rager U, Lippolt P, Hahn A, Fichtner S, Schaefer A, Arseniev L, Ganser A, Drexler H: **Intracoronary bone marrow cell transfer after myocardial infarction: 5-year follow-up from the randomized-controlled BOOST trial.** *Eur Heart J* 2009, **30**:2978-2984.
27. Coghlan C, Hoffman J: **Leonardo da Vinci's flights of the mind must continue: cardiac architecture and the fundamental relation of form and function revisited.** *Eur J Cardiothorac Surg* 2006, **29(Suppl 1)**:S4-17.
28. McDonald IG: **The shape and movements of the human left ventricle during systole. A study by cineangiography and by cineradiography of epicardial markers.** *Am J Cardiol* 1970, **26**:221-230.
29. Helle-Valle T, Remme EW, Lyseggen E, Pettersen E, Vartdal T, Opdahl A, Smith HJ, Osman NF, Ihlen H, Edvardsen T, Smiseth OA: **Clinical assessment of left ventricular rotation and strain: a novel approach for quantification of function in infarcted myocardium and its border zones.** *Am J Physiol Heart Circ Physiol* 2009, **297**:H257-H267.
30. Bertini M, Nucifora G, Marsan NA, Delgado V, van Bommel RJ, Boriani G, Biffi M, Holman ER, van der Wall EE, Schalij MJ, Bax JJ: **Left ventricular rotational mechanics in acute myocardial infarction and in chronic (ischemic and nonischemic) heart failure patients.** *Am J Cardiol* 2009, **103**:1506-1512.
31. Opdahl A, Helle-Valle T, Remme EW, Vartdal T, Pettersen E, Lunde K, Edvardsen T, Smiseth OA: **Apical rotation by speckle tracking echocardiography: a simplified bedside index of left ventricular twist.** *J Am Soc Echocardiogr* 2008, **21**:1121-1128.
32. Garot J, Pascal O, Diebold B, Derumeaux G, Gerber BL, Dubois-Rande JL, Lima JA, Gueret P: **Alterations of systolic left ventricular twist after acute myocardial infarction.** *Am J Physiol Heart Circ Physiol* 2002, **282**:H357-H362.
33. Han W, Xie MX, Wang XF, Lu Q, Wang J, Zhang L, Zhang J: **Assessment of left ventricular torsion in patients with anterior wall myocardial infarction before and after revascularization using speckle tracking imaging.** *Chin Med J (Engl)* 2008, **121**:1543-1548.
34. Ortiz-Perez JT, Rodriguez J, Meyers SN, Lee DC, Davidson C, Wu E: **Correspondence between the 17-segment model and coronary arterial**

anatomy using contrast-enhanced cardiac magnetic resonance imaging. *JACC Cardiovasc Imaging* 2008, **1**:282-293.

35. Ibrahim T, Hackl T, Nekolla SG, Breuer M, Feldmair M, Schomig A, Schwaiger M: **Acute myocardial infarction: serial cardiac MR imaging shows a decrease in delayed enhancement of the myocardium during the 1st week after reperfusion.** *Radiology* 2010, **254**:88-97.
36. Engblom H, Hedstrom E, Heiberg E, Wagner GS, Pahlm O, Arheden H: **Rapid initial reduction of hyperenhanced myocardium after reperfused first myocardial infarction suggests recovery of the peri-infarction zone: one-year follow-up by MRI.** *Circ Cardiovasc Imaging* 2009, **2**:47-55.
37. Orn S, Manhenke C, Anand IS, Squire I, Nagel E, Edvardsen T, Dickstein K: **Effect of left ventricular scar size, location, and transmurality on left ventricular remodeling with healed myocardial infarction.** *Am J Cardiol* 2007, **99**:1109-1114.

doi:10.1186/1532-429X-13-22
Cite this article as: Hopp *et al.*: Regional myocardial function after intracoronary bone marrow cell injection in reperfused anterior wall infarction - a cardiovascular magnetic resonance tagging study. *Journal of Cardiovascular Magnetic Resonance* 2011 **13**:22.

II

III